LA-11288-MS

C.3

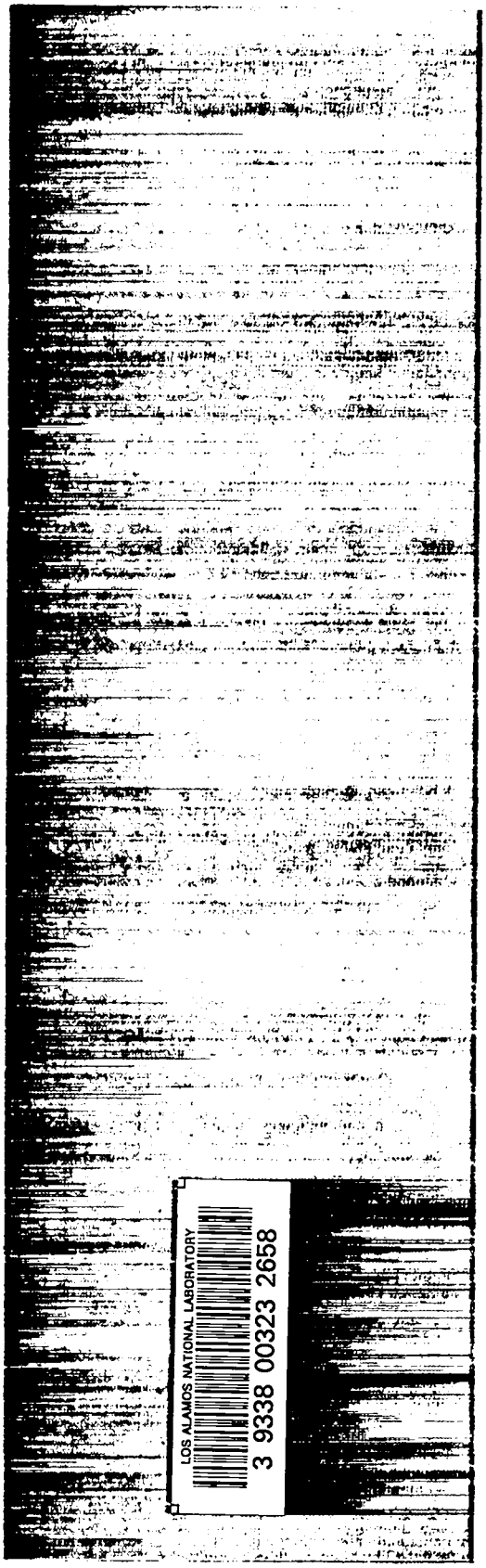

Total and Differential Electron Collision Cross Sections for O_2 and N_2

Los Alamos

Los Alamos National Laboratory is operated by the University of California for the United States Department of Energy under contract W-7405-ENG-36.

An Affirmative Action/Equal Opportunity Employer

LA-11288-MS

UC-34b
Issued: May 1988

Total and Differential Electron Collision Cross Sections for O_2 and N_2

Tim Murphy

Los Alamos National Laboratory
Los Alamos, New Mexico 87545

TOTAL AND DIFFERENTIAL ELECTRON COLLISION CROSS SECTIONS FOR O_2 AND N_2

by

Tim Murphy

Abstract

We present a compilation of total and differential cross sections for electron scattering off N_2 and O_2. Energy-dependent total cross sections and energy- and angle-dependent differential cross sections are given for elastic, rotational, vibrational, electronic excitation, and ionizing collisions.

---

1 Introduction

Electron dynamics plays an important role in the study of the generation and propagation of electromagnetic waves in the atmosphere. One of the most important features of the dynamics, and one of the most difficult to model, is the effect of electron-molecule collisions. Detailed modeling of these effects requires knowledge of the angle- and energy-dependent differential scattering cross sections for a variety of collision processes. Much of this information is published in the literature, but it is widely scattered and not readily available. In the process of developing our KITES kinetic theory atmospheric electron transport computer code, we did a fairly thorough literature search to find the angle- and energy-dependent differential collision cross sections for electrons scattering off N_2 and O_2. We found data for a large number of elastic and inelastic electron collision processes of interest in atmospheric propagation problems. This report describes the differential cross sections used in KITES for elastic, inelastic, and ionizing electron-molecule collisions and explains how these cross sections have been implemented in the code. We hope this information will prove useful to other atmospheric modelers.

Since total cross sections are easier to measure, and hence more accurately known, than differential ones, we use the following general form for the differential cross sections:

$$\frac{d\sigma}{d\Omega}(E,\theta) = A(E,\theta)\frac{\sigma(E)}{4\pi}, \tag{1}$$

$$\int_0^\pi A(E,\theta)\sin\theta d\theta = 2.0, \tag{2}$$

where E is the energy of the incoming electron in eV and θ is the scattering angle in radians. The term $\sigma(E)$ is the total collision cross section and is a function only of energy. The factor A contains all of the angular dependence and is normalized so that Equation (1) will yield the correct total cross section when integrated over all angles. The functional form of A varies with the type of collision being considered.

2 Total Cross Sections

Let us first consider the total cross sections. To implement them in our code we have used actual experimental data where such data were available, using linear interpolation between data points. We consider only collisions with diatomic oxygen and nitrogen, using a composition of 79% nitrogen and 21% oxygen in our model. For elastic, rotational, and vibrational collisions we use experimental results from Phelps[1] and Phelps and Pitchford.[2] The data values used in KITES are listed in Tables 1 through 5. These data extend only to an electron energy of 10 keV, and while rotational and vibrational collision cross sections are not significant above this energy, the elastic cross sections remain appreciable. For elastic collisions with electron energies greater than 10 keV, we use a screened Rutherford cross section,[3] given by

$$\sigma(E) = \frac{2\pi z^2 e^4}{v^2 p^2 \eta(\eta+1)}, \tag{3}$$

$$\eta = \frac{\chi_0^2}{2}\left[1 + 4\alpha z \chi_0 \left(\frac{1-\beta^2}{\beta}\log\chi_0 + \frac{0.231}{\beta} + 1.448\beta\right)\right], \tag{4}$$

$$\chi_0 = \frac{\hbar\mu}{p}\frac{z^{1/3}}{0.885 a_0}, \tag{5}$$

where z is the average atomic number of air, e is the electron charge in esu, v is the electron velocity, p is the electron momentum, $\beta = v/c$, α is the fine-structure constant, a_o is the Bohr radius of the electron, and μ is an adjustable parameter. Matching this formula to the cross-section data at 10 keV yields a value of $\mu = 0.635$. The elastic, rotational, and vibrational cross sections are shown in Figures 1 through 5.

Table 1: N_2 TOTAL ELASTIC CROSS SECTIONS

E (ev)	$\sigma(10^{-16}cm^2)$	E (ev)	$\sigma(10^{-16}cm^2)$
0.0	1.1	2.5	19.11
0.001	1.33	2.8	22.7
0.002	1.436	3.0	18.74
0.003	1.539	3.3	16.88
0.005	1.675	3.6	15.59
0.007	1.811	4.0	14.08
0.0085	1.87	4.5	12.9
0.01	1.92	5.0	12.74
0.015	2.23	6.0	12.53
0.02	2.49	7.0	12.43
0.03	2.95	8.0	13.01
0.04	3.35	10.0	13.23
0.05	3.78	12.0	13.23
0.07	4.48	15.0	12.8
0.10	5.26	17.0	12.56
0.12	5.72	20.0	12.1
0.15	6.33	25.0	11.41
0.17	6.62	30.0	10.67
0.2	7.11	50.0	8.3
0.25	7.7	75.0	6.66
0.3	8.22	100.0	5.38
0.35	8.62	150.0	4.18
0.4	8.96	200.0	3.5
0.5	9.24	300.0	2.7
0.7	9.52	500.0	1.831
1.0	9.74	700.0	1.455
1.2	10.26	1000.0	1.029
1.3	10.91	1500.0	0.744
1.5	11.99	2000.0	0.538
1.7	13.78	3000.0	0.418
1.9	16.98	5000.0	0.266
2.1	17.62	7000.0	0.193
2.2	18.94	10000.0	0.14

Table 2: O_2 TOTAL ELASTIC CROSS SECTIONS

E (ev)	$\sigma(10^{-16}cm^2)$	E (ev)	$\sigma(10^{-16}cm^2)$
0.0	0.35	2.5	6.1
0.001	0.35	2.8	5.8
0.002	0.36	3.0	5.7
0.003	0.4	3.3	5.5
0.005	0.5	3.6	5.45
0.007	0.58	4.0	5.5
0.0085	0.64	4.5	5.55
0.01	0.7	5.0	5.6
0.015	0.87	6.0	6.0
0.02	0.99	7.0	6.6
0.03	1.24	8.0	7.1
0.04	1.44	10.0	8.0
0.05	1.6	12.0	8.5
0.07	2.1	15.0	8.8
0.10	2.5	17.0	8.7
0.12	2.8	20.0	8.6
0.15	3.1	25.0	8.2
0.17	3.3	30.0	8.
0.2	3.6	50.0	7.7
0.25	4.1	75.0	6.8
0.3	4.5	100.0	6.5
0.35	4.7	150.0	4.99
0.4	5.2	200.0	4.14
0.5	5.7	300.0	3.18
0.7	6.1	500.0	2.28
1.0	7.2	700.0	1.83
1.2	7.9	1000.0	1.45
1.3	7.9	1500.0	1.14
1.5	7.6	2000.0	0.828
1.7	7.3	3000.0	0.638
1.9	6.9	5000.0	0.395
2.1	6.6	7000.0	0.289
2.2	6.5	10000.0	0.209

Table 3: O_2 TOTAL ROTATIONAL CROSS SECTION

E (ev)	$\sigma(10^{-16}cm^2)$	E (ev)	$\sigma(10^{-16}cm^2)$
0.0	0.0	0.91	0.084
0.0067	0.0	0.93	0.0
0.07	0.0	1.02	0.0
0.08	0.0054	1.03	0.0720
0.1	0.0	1.05	0.0
0.2	0.0	1.13	0.0
0.21	0.0216	1.14	0.0468
0.22	0.0	1.16	0.0
0.32	0.0	1.23	0.0
0.33	0.384	1.24	0.06
0.35	0.0	1.26	0.0
0.44	0.0	1.34	0.0
0.45	0.054	1.35	0.0360
0.47	0.0	1.37	0.0
0.56	0.0	1.44	0.0
0.57	0.672	1.45	0.024
0.59	0.0	1.47	0.0
0.68	0.0	1.54	0.0
0.69	0.0804	1.55	0.012
0.71	0.0	1.57	0.0
0.79	0.0	1.64	0.0
0.80	0.0936	1.65	0.0048
0.81	0.0	1.67	0.0
0.90	0.0		

Table 4: N_2 TOTAL ROTATIONAL CROSS SECTION

E (ev)	$\sigma(10^{-16}cm^2)$	E (ev)	$\sigma(10^{-16}cm^2)$
0.0	0.0	2.4	2.19
0.02	0.0	2.5	2.4
0.03	0.025	2.6	2.17
0.40	0.025	2.7	1.62
0.80	0.025	2.8	1.38
1.2	0.047	2.9	1.18
1.6	0.086	3.0	1.03
1.7	0.015	3.1	0.84
1.8	0.235	3.2	0.69
1.9	1.08	3.3	0.50
2.0	1.90	3.6	0.17
2.1	2.03	5.0	0.0
2.2	2.77	20.0	0.0
2.3	2.5		

Table 5: N_2 TOTAL VIBRATIONAL CROSS SECTION

E (ev)	$\sigma(10^{-16}cm^2)$	E (ev)	$\sigma(10^{-16}cm^2)$
0.0	0.0	2.4	8.055
1.0	0.0	2.5	9.705
1.1	0.0044	2.6	6.96
1.16	0.0053	2.7	7.095
1.2	0.0060	2.75	7.095
1.22	0.0066	2.8	5.775
1.4	0.0345	2.9	3.72
1.5	0.0480	3.0	3.33
1.6	0.0660	3.1	2.265
1.65	0.0780	3.2	1.695
1.7	0.0915	3.3	1.125
1.8	0.1650	3.4	0.45
1.9	0.8025	3.5	0.2955
2.0	3.3750	3.6	0.1650
2.1	4.74	4.0	0.0
2.2	6.57	100.0	0.0
2.3	7.725	1000.0	0.0

For the electronic excitations we use the fits given in Banks and Kockarts,[4] with one addition and some modifications. The formula used for the cross sections is

$$\sigma(E) = (q_0 c_0 f_0 / W^2)[1 - (W/E)^\gamma]^\nu (W/E)^\Omega \quad cm^2, \tag{6}$$

where $q_0 = 6.51 \times 10^{-14}$ eV^{2}cm^2 and W is the threshold energy in eV. In addition to the reactions listed in Banks and Kockarts' Table 9.5, we have included the $W^3\Delta_u$ state for nitrogen. Since the threshold energy for this state is within 0.01 eV of that of the $B^3\Pi_g$ state, we have simply combined the cross sections for these two reactions. A comparison with the experimental data of Cartwright et al.[5] for a subset of the reactions listed in Banks and Kockarts led us to revise some of the cross-section fit parameters in the table. The values used in KITES are listed in Table 6. Plots of the cross sections are shown in Figures 6 through 18.

Table 6: ELECTRON IMPACT EXCITATION CROSS SECTION PARAMETERS

Gas	State	W	$c_0 f_0$	Ω	ν	γ
N_2	$A^3\Sigma_u^+$	6.17	0.1912	2.0	4.0	1.8
	$B^3\Pi_g + W^3\Delta_u$	7.36	1.0900	2.8	4.0	2.0
	$C^3\Pi_u$	11.03	0.4453	4.0	1.5	3.0
	$a^1\Pi_g$	8.55	0.4698	1.8	2.0	1.0
	$b^1\Pi_u$	12.85	1.5100	0.75	3.0	1.0
	$bl^1\Sigma_u^+$	14.0	0.33	0.75	3.0	1.0
	Σ Rydberg	13.75	2.66	0.75	3.0	1.0
O_2	$a^1\Delta_g$	0.98	0.0005	3.0	1.0	3.0
	$b^1\Sigma_g$	1.64	0.0005	3.0	1.0	3.0
	$A^3\Sigma_u^+$	4.5	0.021	0.9	1.0	3.0
	$B^3\Sigma_u^-$	8.4	0.23	0.75	2.0	1.0
	9.9 eV allowed	9.9	0.08	0.75	3.0	1.0
	Σ Rydberg	13.5	2.77	0.75	3.0	1.0

For ionizing collisions with incident electrons of energy up to 15 keV, we use data from the cross-section measurements of Rapp and Englander-Golden [6] and Opal, Beaty and Peterson.[7,8] Their results are given in Tables 7 and 8. For incident electrons with energy above 15 keV, we use a formula from a paper by Longmire and Longley,[9] which is in turn based on a calculation by Bethe.[10] The high-energy ionization cross section is given by

$$\sigma(E) = 5.94 \times 10^{-20} \frac{\gamma^2}{\gamma^2 - 1}[8.68 + \log(\gamma^2 - 1) + \frac{1}{\gamma^2}] \quad cm^2, \tag{7}$$

where E is the kinetic energy of the electron and γ is the usual relativistic factor, given by

$$\gamma = 1 + \frac{E}{mc^2}. \tag{8}$$

The cross sections are shown in Figures 19 and 20.

Table 7: N_2 TOTAL IONIZATION CROSS SECTION

E (ev)	$\sigma(10^{-16}cm^2)$	E (ev)	$\sigma(10^{-16}cm^2)$
0.0	0.0	45.0	1.776
15.6	0.0	60.0	2.18
16.0	0.0211	75.0	2.391
16.5	0.0466	100.0	2.5227
17.0	0.0712	150.0	2.452
17.5	0.0984	200.0	2.268
18.0	0.129	300.0	1.916
18.5	0.163	500.0	1.4504
19.0	0.1987	700.0	1.1603
19.5	0.230	1000.0	0.923
20.0	0.2699	1500.0	0.744
21.0	0.3437	2000.0	0.4836
22.0	0.4175	3000.0	0.3534
23.0	0.4914	5000.0	0.2139
25.0	0.639	7000.0	0.1581
30.0	1.0284	10000.0	0.1116
34.0	1.266	15000.0	0.0698

Table 8: O_2 TOTAL IONIZATION CROSS SECTION

E (ev)	$\sigma(10^{-16}cm^2)$	E (ev)	$\sigma(10^{-16}cm^2)$
0.0	0.0	45.0	1.696
12.6	0.0	60.0	2.171
15.5	0.0984	75.0	2.461
16.0	0.1143	100.0	2.672
16.5	0.1362	150.0	2.690
17.0	0.1582	200.0	2.532
17.5	0.1802	300.0	2.180
18.0	0.2030	500.0	1.6701
18.5	0.2285	700.0	1.345
19.0	0.2532	1000.0	1.055
19.5	0.2786	1500.0	0.8504
20.0	0.3068	2000.0	0.5528
21.0	0.3595	3000.0	0.4040
22.0	0.4158	5000.0	0.2445
24.0	0.5344	7000.0	0.1807
26.0	0.6540	10000.0	0.1275
30.0	0.8966	15000.0	0.07975
34.0	1.151		

3 Differential Cross Sections

Now we shall consider the various forms of the function A defined above. Because this function has to integrate to exactly 2.0, we have used fits to the data, which we can normalize precisely.

For elastic collisions we use the data of Shyn, Stolarski, and Carignan, [11] and we find a fit of the form

$$A(E,\theta) = \frac{4N\eta_1(1+\eta_1)}{(1-\cos\theta+2\eta_1)^2} + \frac{4(1-N)\eta_2(1+\eta_2)}{(1+\cos\theta+2\eta_2)^2}, \tag{9}$$

where

$$\eta_1 = 5.77E^{-1.377}, \tag{10}$$

$$\eta_2 = 2.64E^{-0.8964}. \tag{11}$$

The factor N is also energy dependent, but we were not able to find a simple expression for it. The values used in our code are tabulated in Section 4.

For inelastic collisions there is not a great deal of data available on differential cross sections. For rotational excitations we use data from Wong and Dubé,[12] and for vibrational excitations we use results from Polak and Slovetskii.[13] Both sets of data are fit by the formula

$$A(E,\theta) = \frac{15}{14}(1 - 3\cos^2\theta + \frac{14}{3}\cos^4\theta). \tag{12}$$

The angular behavior of the cross sections for the various electronic states varies quite a bit, and we could not find data for many of the states included in the table from Banks and Kockarts mentioned above. We were able to find results for some of the reactions in a paper by Cartwright et al., [14] and found fits of the following forms:

$$N_2 \quad A^3\Sigma_u^+ : \quad A(E,\theta) = 0.207 + \frac{0.138}{0.25 + (\frac{\pi}{2} - \theta)^2} + 3.244e^{1.5(\theta-\pi)}, \tag{13}$$

$$N_2 \quad B^3\Pi_g : \quad A(E,\theta) = \frac{1.374}{0.8 + (\frac{3\pi}{4} - \theta)^2}, \tag{14}$$

$$N_2 \quad a^1\Pi_g : \quad A(E,\theta) = 0.2947 + 9.5286e^{-2.4\theta}, \tag{15}$$

$$N_2 \quad C^3\Pi_u : \quad A(E,\theta) = \frac{8.2712}{4.0 + (\pi - \theta)^2} - 0.3102. \tag{16}$$

For the angular behavior of the cross sections for the Rydberg states we use a formula developed by Phelps and Pitchford:[15]

$$A(E,\theta) = 1.0 + \sum_{i=1}^{5} c_i P_i(\cos\theta), \tag{17}$$

where the coefficients c_i are given by

$$c_1 = \frac{E^2}{2500 + E^2}, \tag{18}$$

$$c_2 = \frac{E^2}{2500 + E^2}, \tag{19}$$

$$c_3 = \frac{E^2}{3500 + E^2}, \tag{20}$$

$$c_4 = \frac{E^2}{3500 + E^2}, \tag{21}$$

$$c_5 = \frac{E^2}{3500 + E^2}. \tag{22}$$

All other inelastic cross sections are considered to be isotropic.

For ionizing collisions the situation is a bit more complicated because the cross sections are functions of both the secondary electron energy and the scattering angle. We factor the angle-dependent term A in Equation (1) into two parts, one dependent only on the incoming electron energy E and the secondary electron energy $\mathcal{E}$ and the other dependent only on $\mathcal{E}$ and the scattering angle θ. The energy-dependent term $B(E, \mathcal{E})$ is normalized to integrate to 1.0, and the angular term $\mathcal{A}(\mathcal{E}, \theta)$ integrates to 2.0 as before. For both terms we use fits to the data of Opal, Beaty, and Peterson,[7,8] with the angular modification factor suggested by DuBois and Rudd.[16] Opal, Beaty, and Peterson only measured the cross sections out to secondary electron energies equal to half of the energy of the incoming electron, so we cannot use their data directly for secondary electrons above this energy. The behavior of the energy-dependent term B over the remainder of the range of secondary electron energies can be inferred by energy conservation, however; and we find a fit of the form

$$B(E, \mathcal{E}) = \frac{1}{a \arctan\left(\frac{E-b}{2a}\right)} \begin{cases} \dfrac{1}{1.0 + \left(\frac{\mathcal{E}}{a}\right)^{2.1}} & \mathcal{E} \leq \frac{E-b}{2} \\ \dfrac{1}{1.0 + \left(\frac{E-b-\mathcal{E}}{a}\right)^{2.1}} & \frac{E-b}{2} < \mathcal{E} < E - b \end{cases} \tag{23}$$

where b is the threshold energy for ionization. For nitrogen we have a=13.0 eV and b=15.6 eV, while for oxygen the values are a=17.25 eV and b=12.6 eV.

The angle-dependent term $\mathcal{A}$ is more difficult. As mentioned above, Opal et al. did not measure $\mathcal{A}$ for secondary electron energies above half of the incident electron energy, and its behavior for the higher energy secondary electrons cannot be inferred from that of the lower energy electrons. Dubois and Rudd did measure the angle-dependent ionization cross sections for electrons on nitrogen and oxygen up to the maximum possible secondary electron energy, but their data are quoted for only a few angular points, and one cannot reconstruct the angular dependence from them. Forced to

make an educated guess, we decided to use the angular fit for elastic scattering for the secondary electrons with an energy greater than half the energy of the incoming electrons. For the secondary electrons with less than half the incoming energy, we have

$$A(\mathcal{E},\theta) = N_1 + N_2 e^{-\frac{(\theta-c)^2}{w^2}}, \tag{24}$$

where N_1, N_2, c, and w are energy-dependent parameters. We were not able to find simple analytic expressions for these parameters, and the values used in KITES are listed in Section 4.

4 Implementation of the Cross Sections

We have found that the angle-dependent term $A(E,\theta)$ in Equation (1) varies much more slowly with energy than does the total cross-section term $\sigma(E)$. In evaluating the differential cross sections for use in our computer code we therefore calculate $\sigma(E)$ for each energy in the problem but evaluate $A(E,\theta)$ only at selected energies. We use linear interpolation to estimate the angular dependence at energy values between those selected. The number of energies selected and their values depend on the type of collision being considered. This section describes the choices made in implementing the differential cross sections in KITES.

For elastic collisions we calculate the angle-dependent term $A(E,\theta)$ at 10 energies between 5 and 10,000 eV. The fit parameters for each energy are

Energy (eV)	N	η_1	η_2
5	0.67	0.63	0.62
10	0.60	0.24	0.34
15	0.60	0.14	0.23
20	0.75	0.093	0.18
30	0.80	0.053	0.13
50	0.85	0.026	0.079
100	0.95	0.010	0.043
500	1.00	$1.11e^{-3}$	0.010
1000	1.00	$4.27e^{-4}$	$5.40e^{-3}$
10000	1.00	$1.79e^{-5}$	$6.85e^{-4}$

For inelastic collisions the total cross sections are generally so sharply peaked in energy that one can just use the angular distribution at the peak of the cross section and calculate a single $A(E,\theta)$. The exception is the excitation of Rydberg states, for which we must calculate the angular dependence for several energies as was done for the elastic collisions. The fits are evaluated at the following energies:

vibrational	2 eV
rotational	2 eV
$A^3\Sigma_u^+$	17 eV
$B^3\Pi_g + W^3\Delta_u$	15 eV
$a^1\Pi_g$	17 eV
$C^3\Pi_u$	15 eV
Rydberg	20, 50, 100, 1000 eV

For ionizing collisions we calculate the energy-dependent factor B at each secondary electron energy. The angular factor A is evaluated for five secondary electron energies. We find for the parameters:

E (eV)	N_1	N_2	c	w
4.13	1.0928	-0.1366	1.80	1.0
20.1	0.7682	0.5122	0.70	0.9
48.5	0.5988	0.8982	0.80	0.8
98.0	0.4546	1.3636	0.80	0.7
196.0	0.3140	2.1020	0.90	0.5

The angle dependent factors $A(E,\theta)$ described above are shown in Figures 21 through 46.

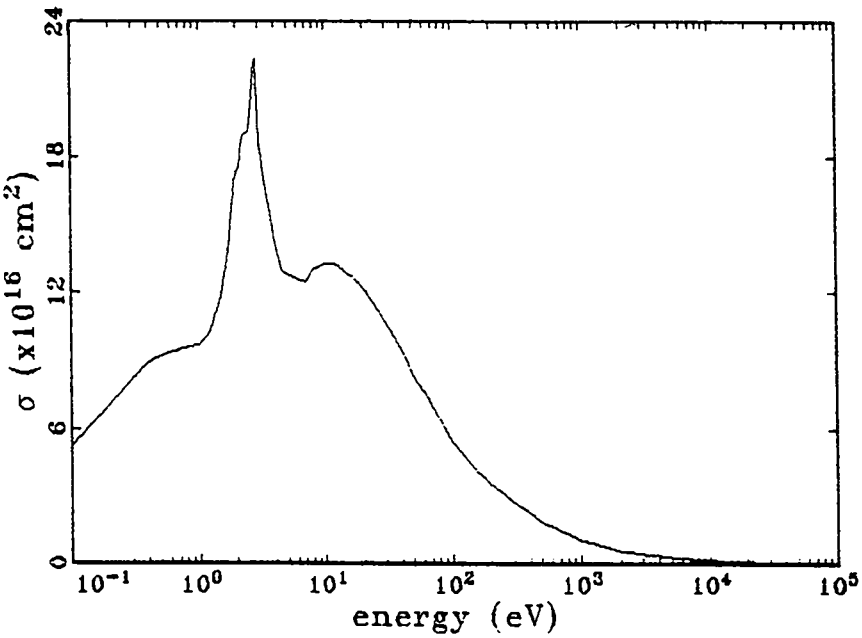

Figure 1: N_2 elastic total cross section.

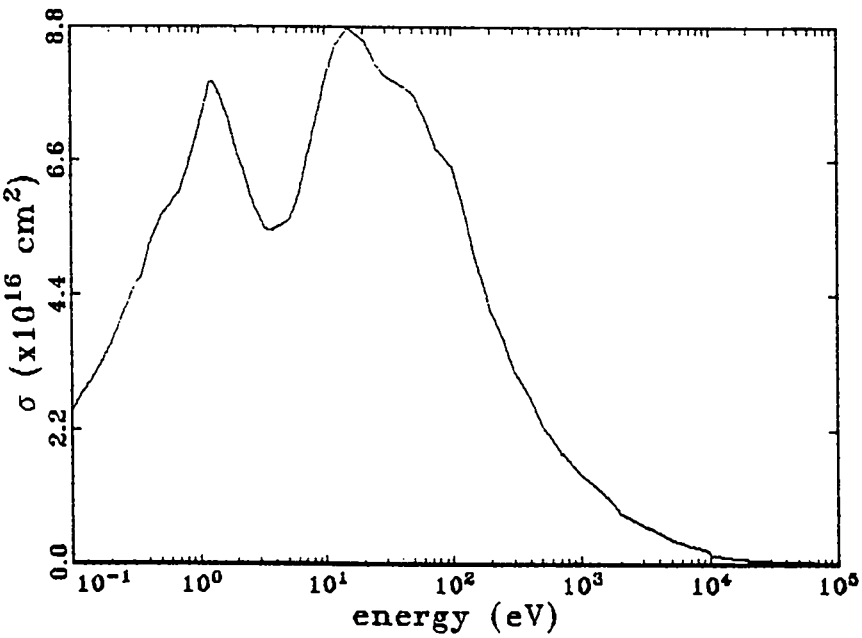

Figure 2: O_2 elastic total cross section.

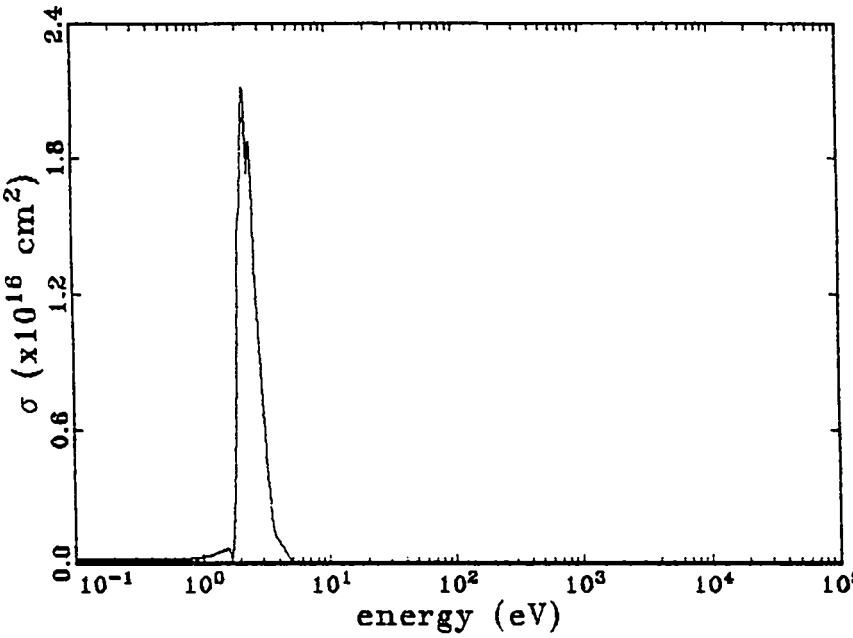

Figure 3: N_2 rotational total cross section.

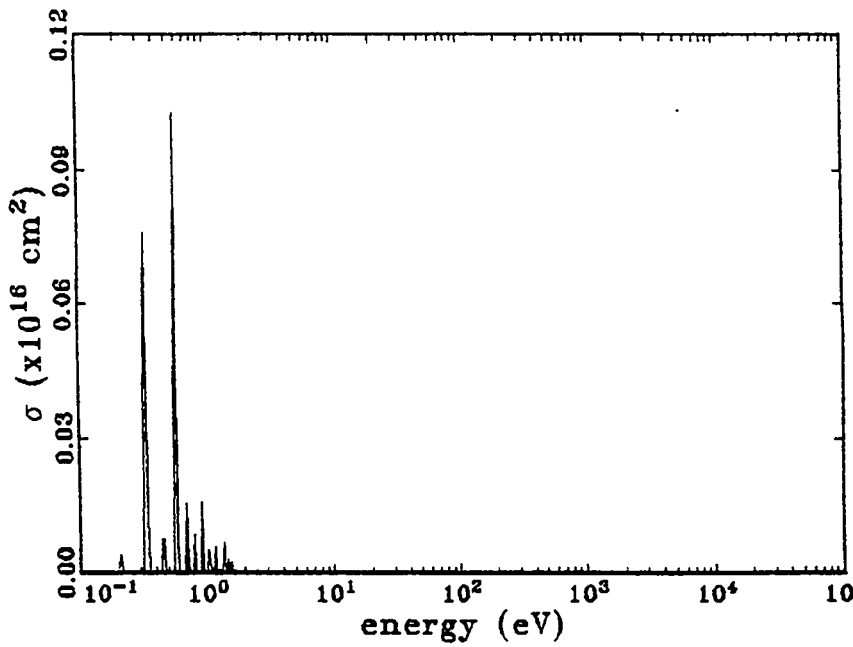

Figure 4: O_2 rotational total cross section.

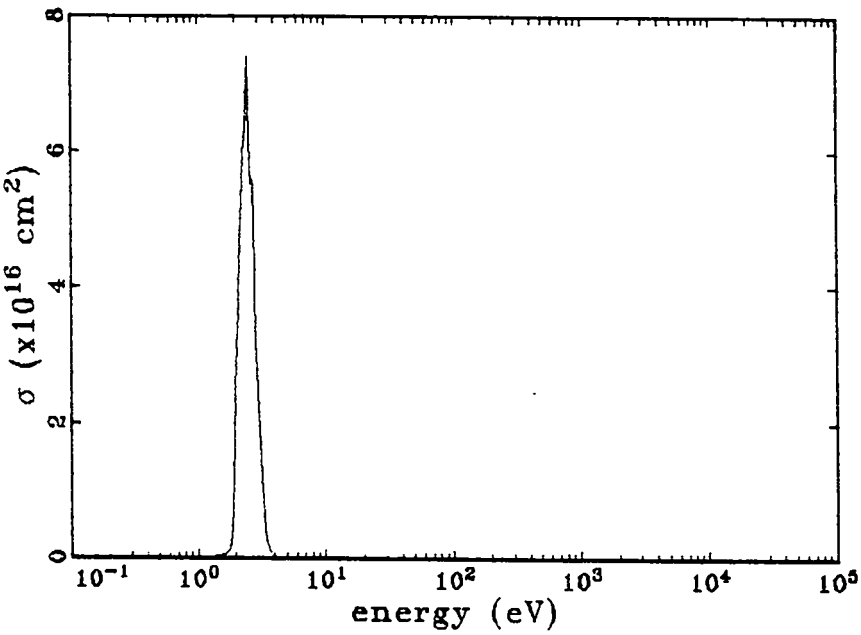

Figure 5: N_2 vibrational total cross section.

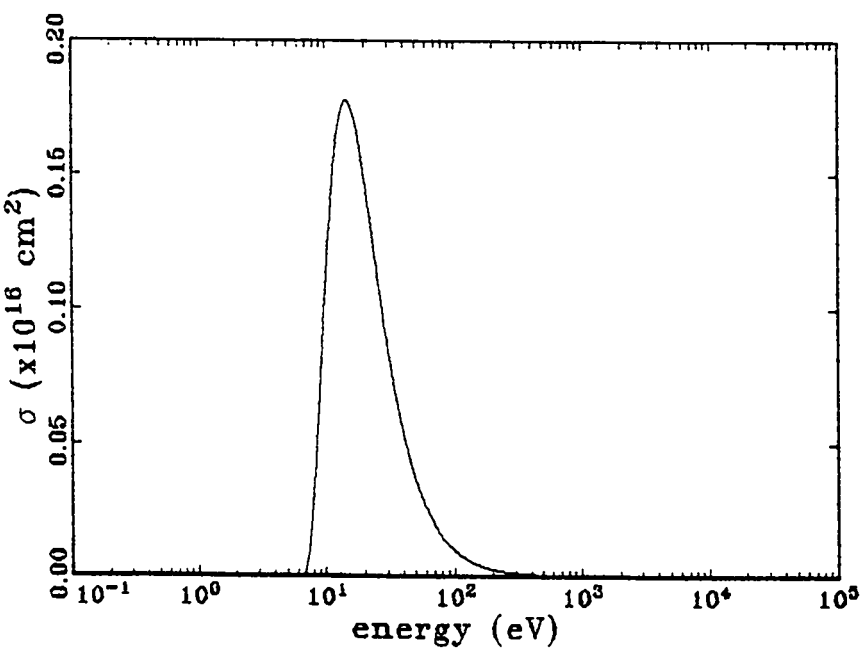

Figure 6: N_2 $A^3\Sigma_u^+$ total cross section.

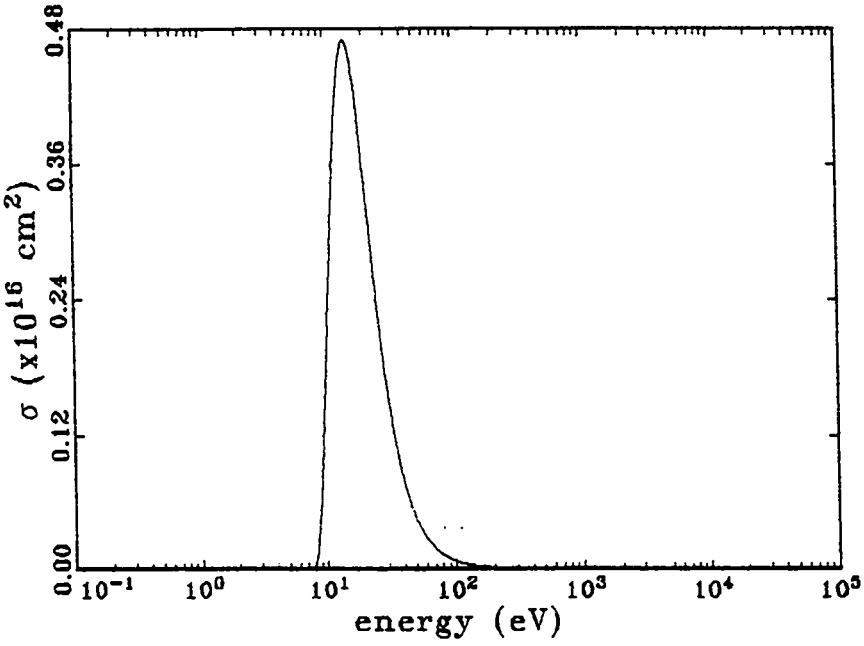

Figure 7: N_2 $B^3\Pi_g + W^3\Delta_u$ total cross section.

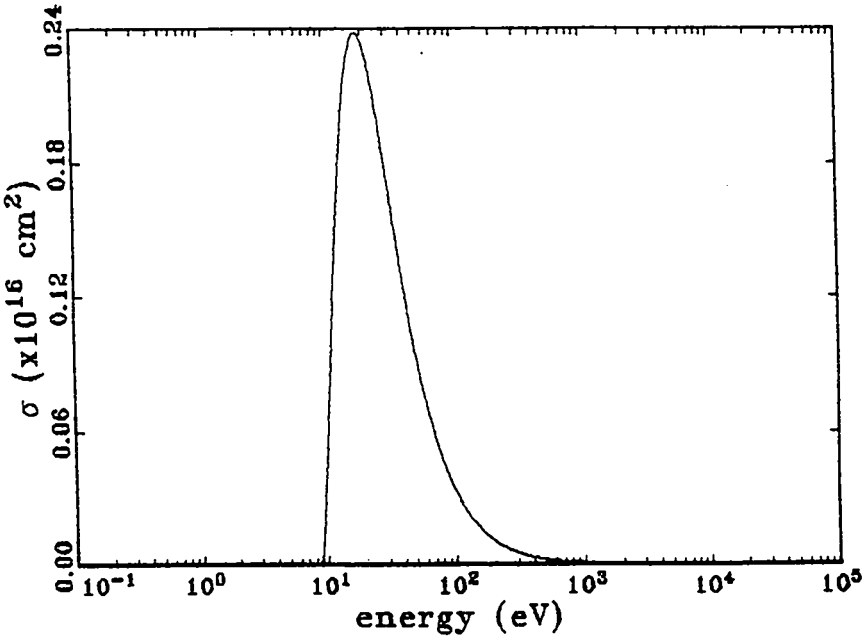

Figure 8: N_2 $a^1\Pi_g$ total cross section.

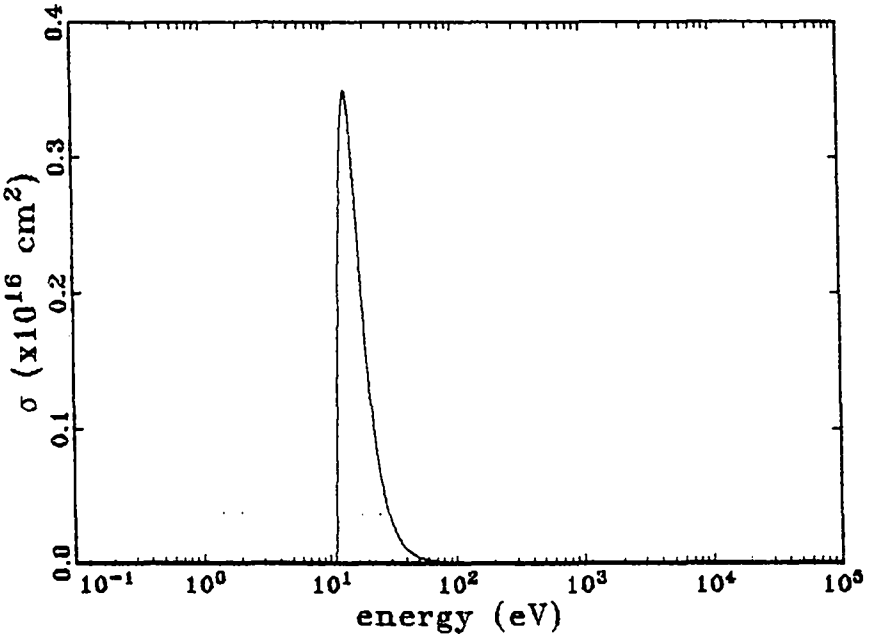

Figure 9: N_2 $C^3\Pi_u$ total cross section.

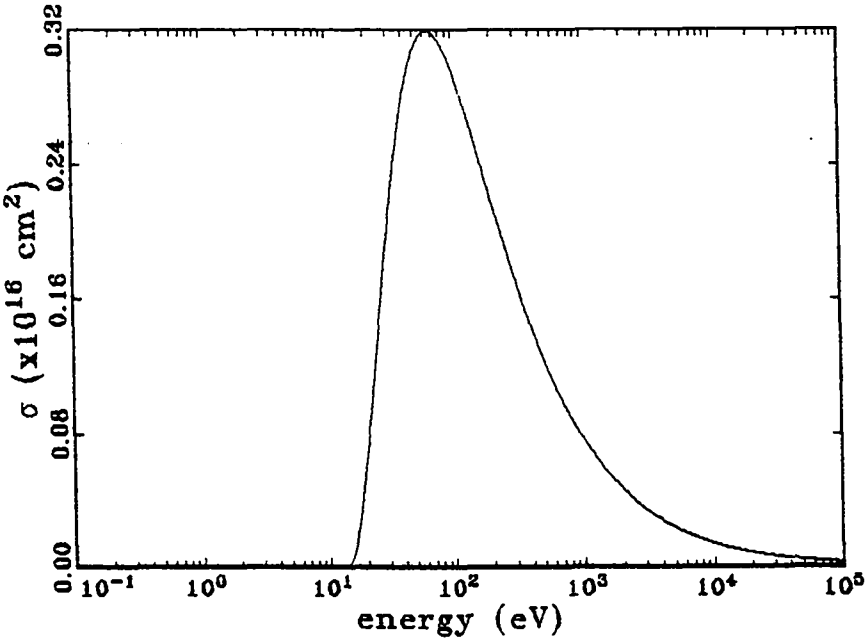

Figure 10: N_2 $b^1\Pi_u$ total cross section.

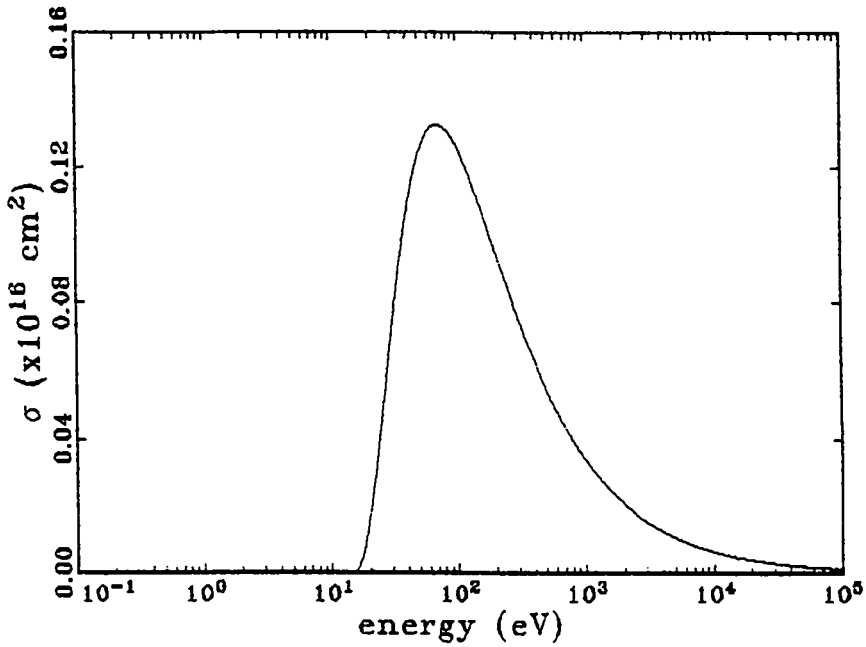

Figure 11: N_2 $b^1\Sigma_u^+$ total cross section.

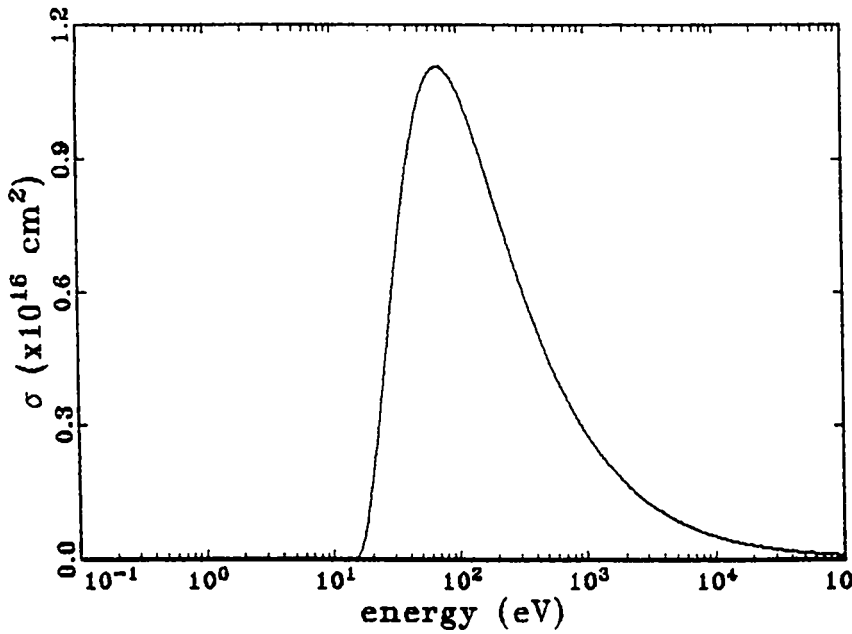

Figure 12: N_2 Σ Rydberg total cross section.

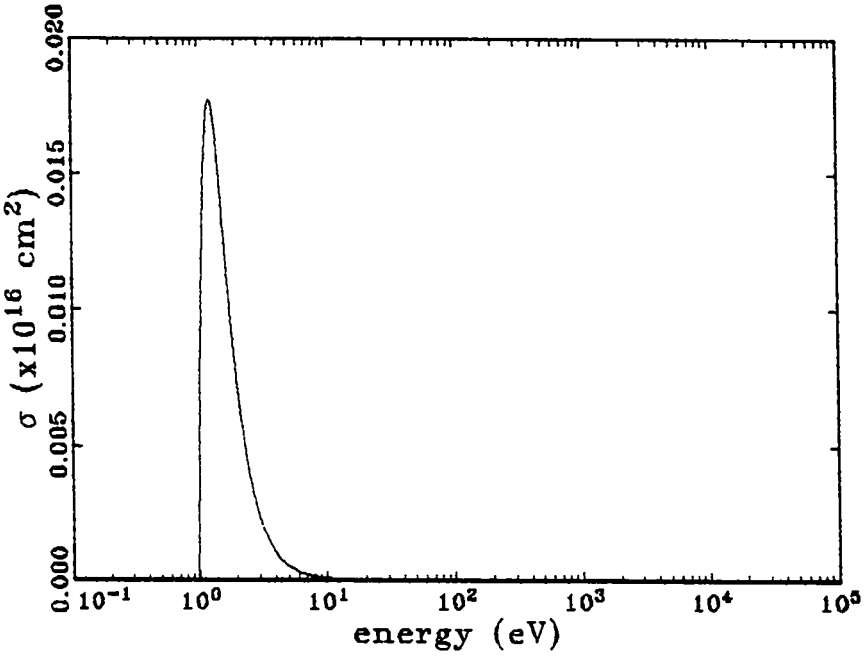

Figure 13: O_2 $a^1\Delta_g$ total cross section.

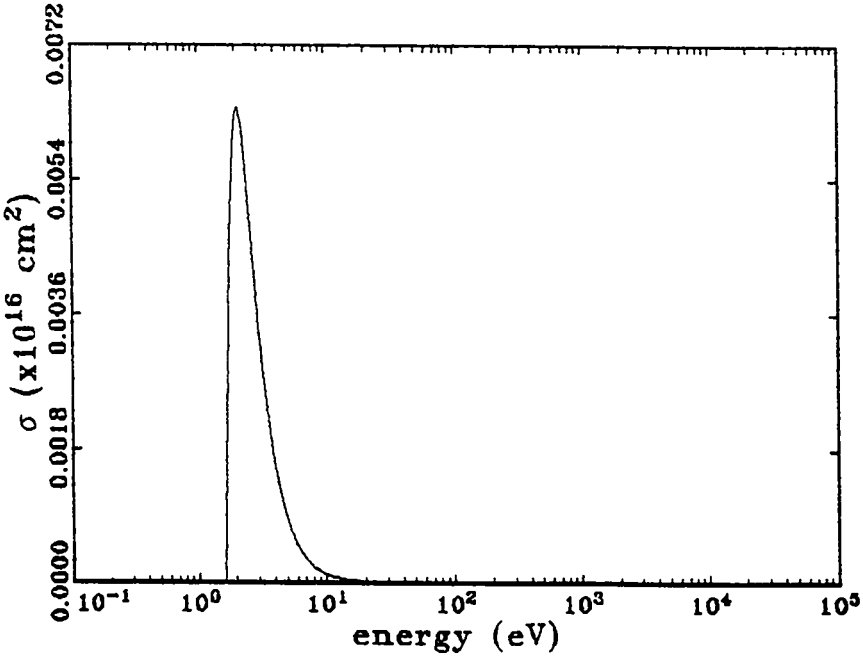

Figure 14: O_2 $b^1\Sigma_g$ total cross section.

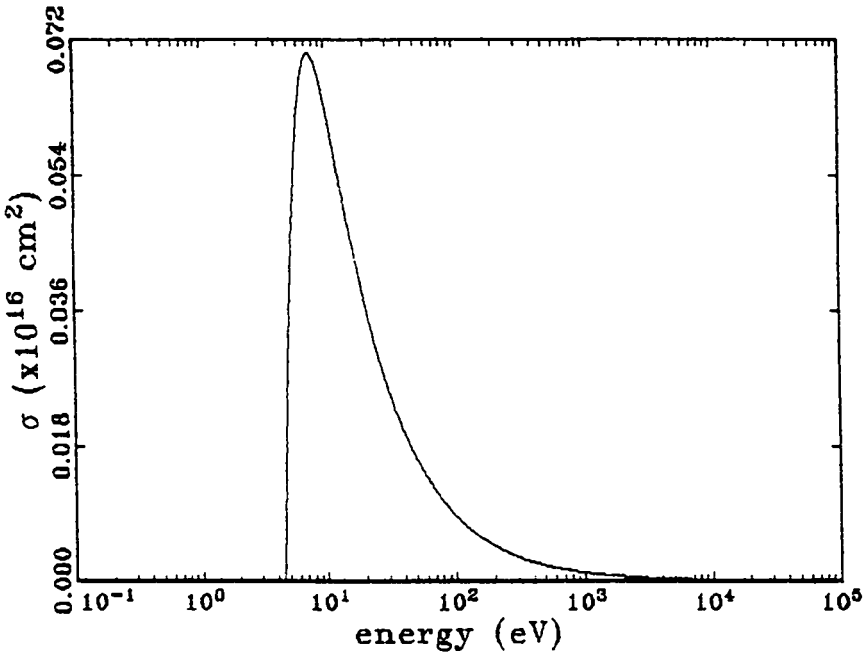

Figure 15: O_2 $A^3\Sigma_u$ total cross section.

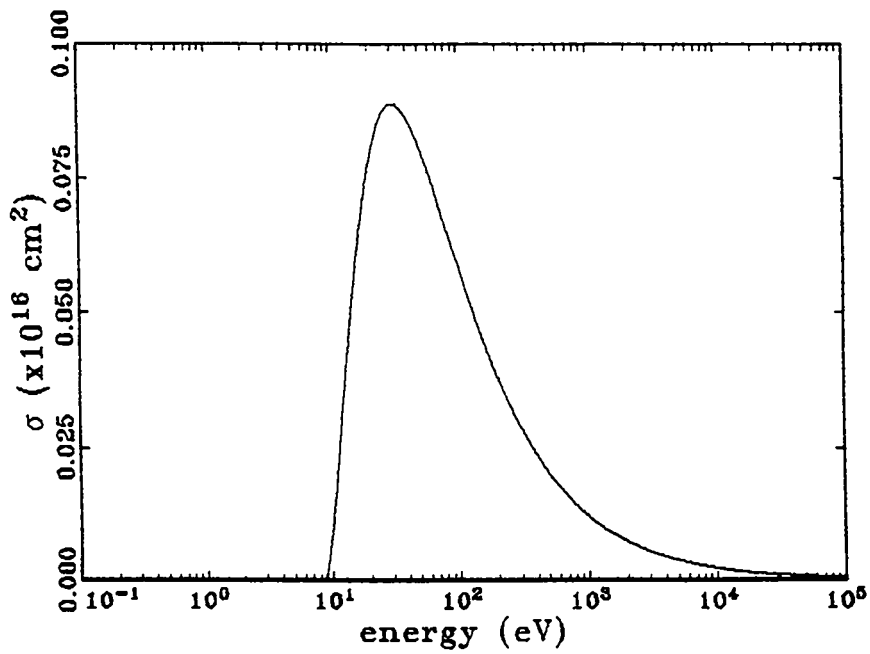

Figure 16: O_2 $B^3\Sigma_u^-$ total cross section.

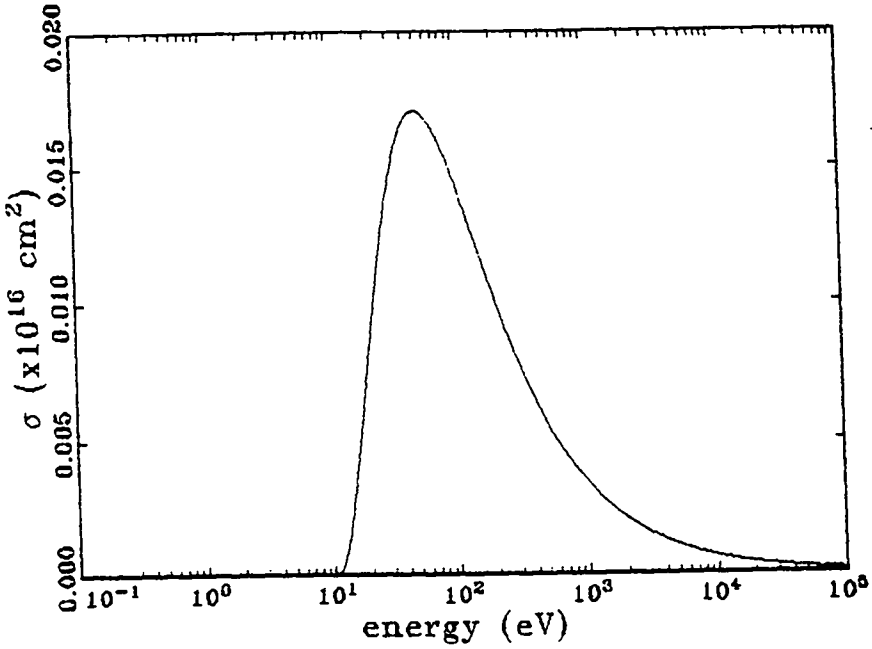

Figure 17: O_2 9.9-eV allowed total cross section.

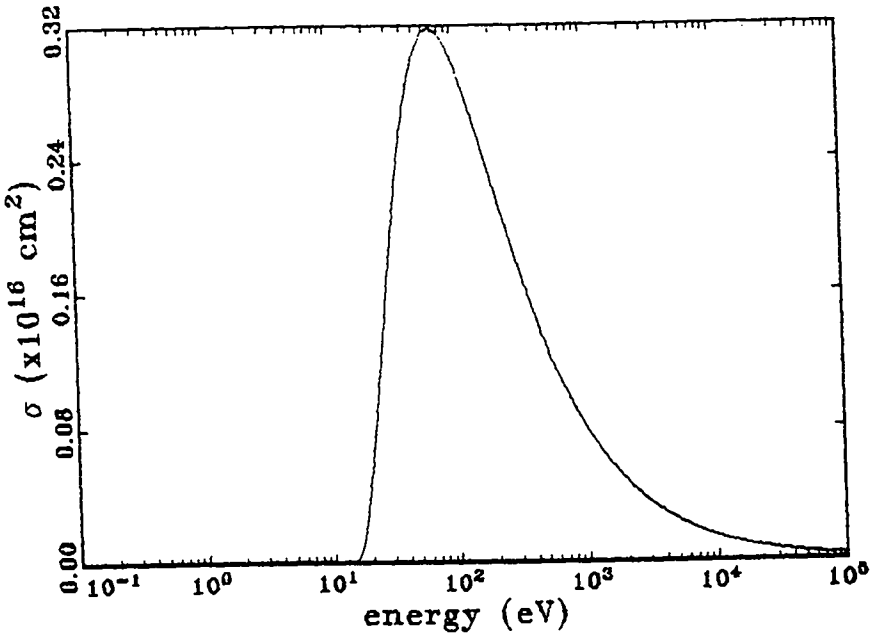

Figure 18: O_2 Σ Rydberg total cross section.

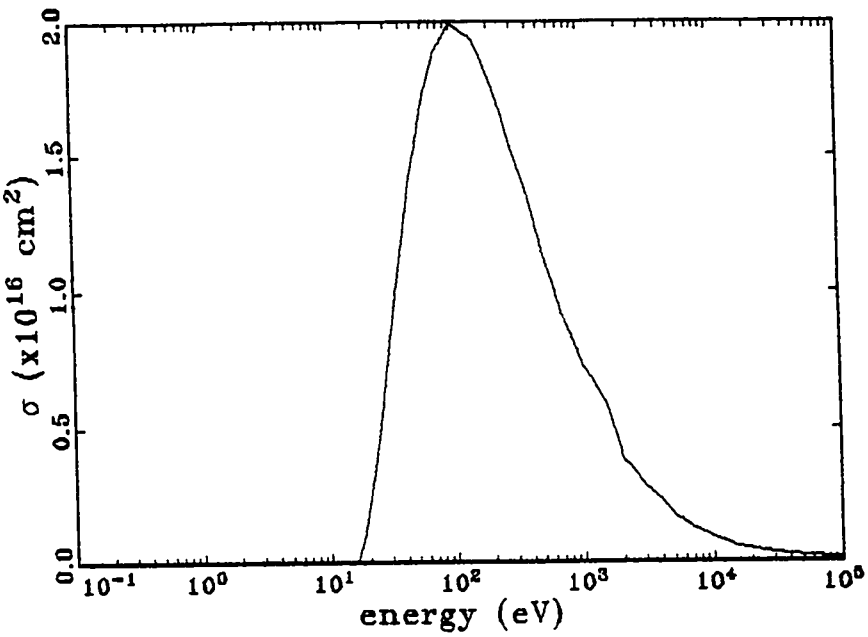

Figure 19: N_2 ionization total cross section.

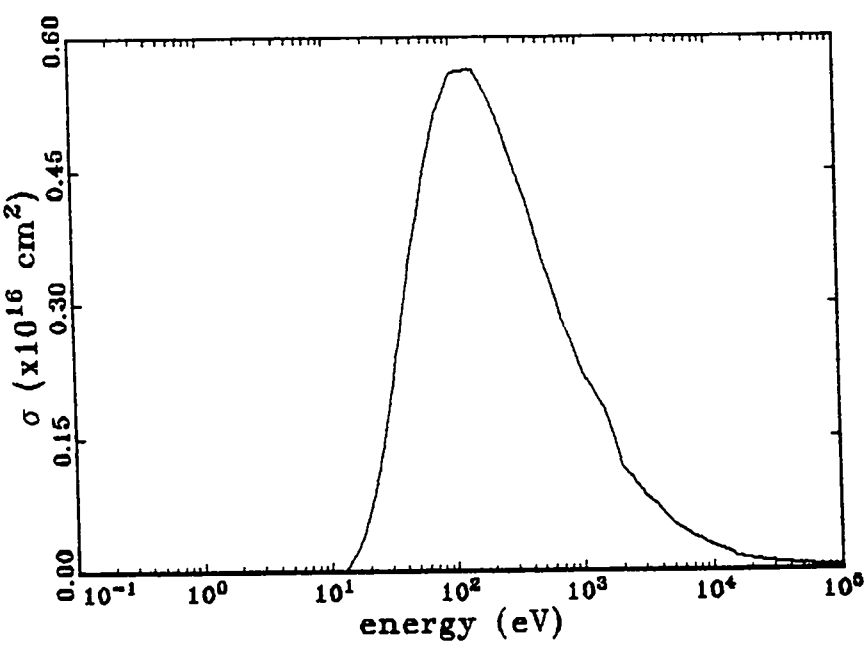

Figure 20: O_2 ionization total cross section.

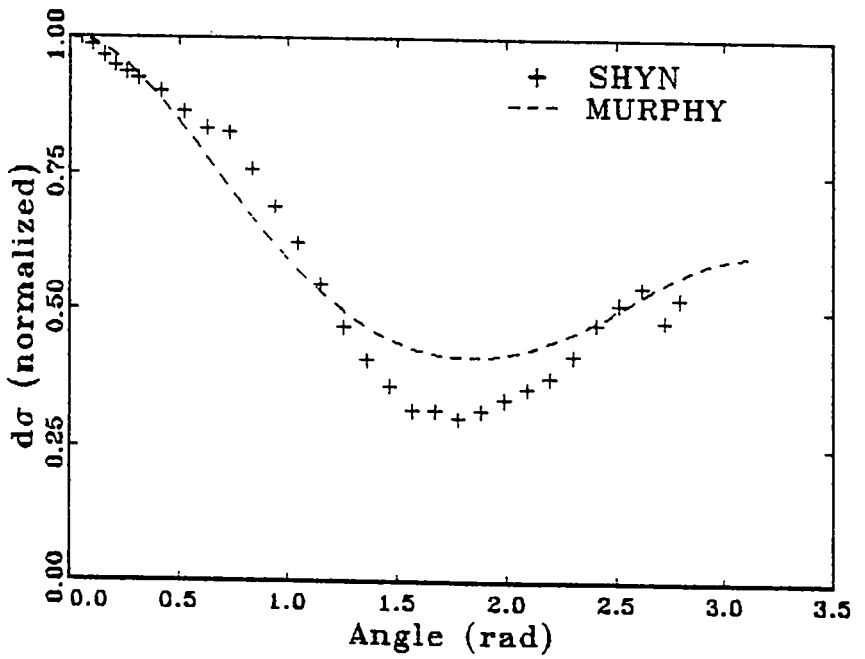

Figure 21: Elastic differential cross section at 5 eV.

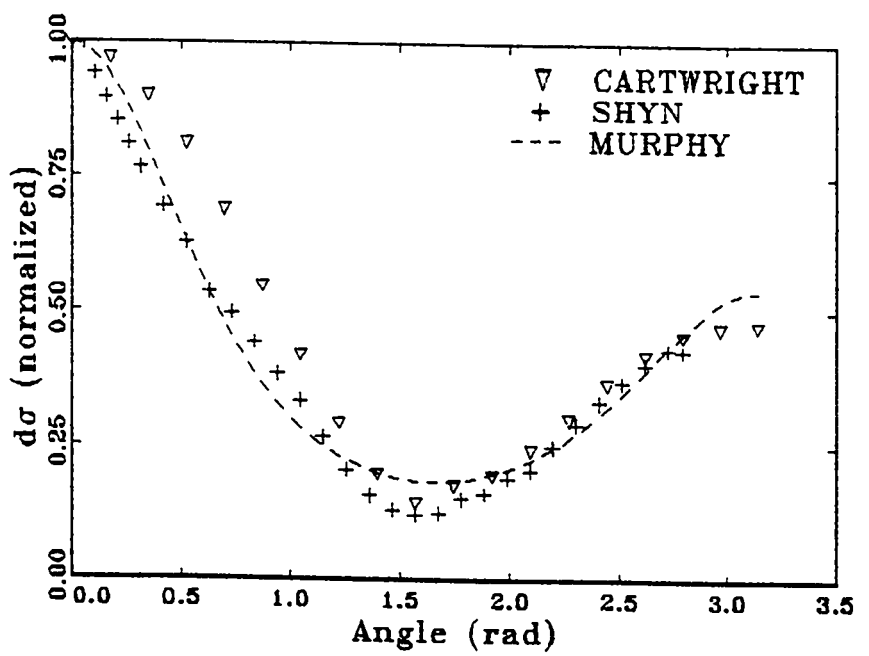

Figure 22: Elastic differential cross section at 10 eV.

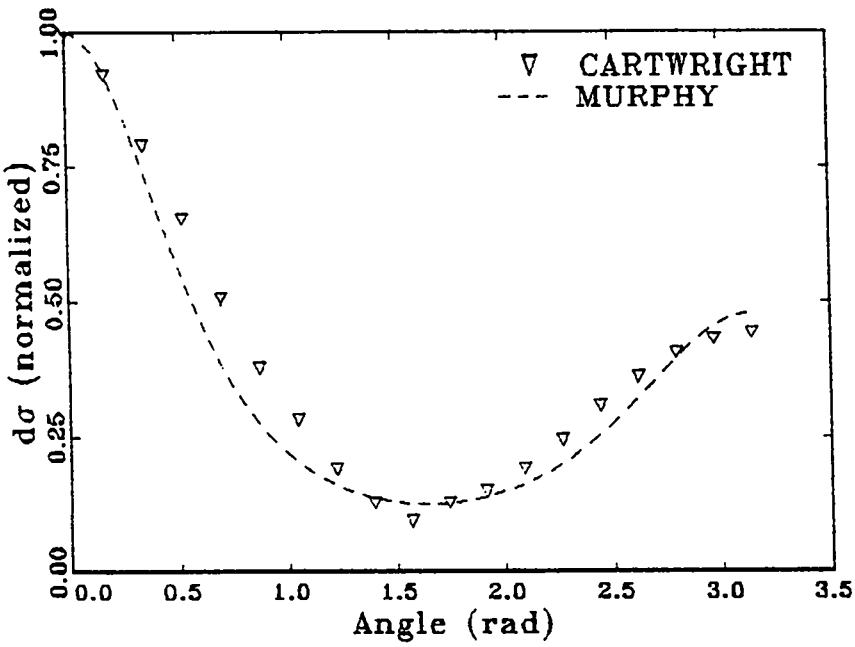

Figure 23: Elastic differential cross section at 12.5 eV.

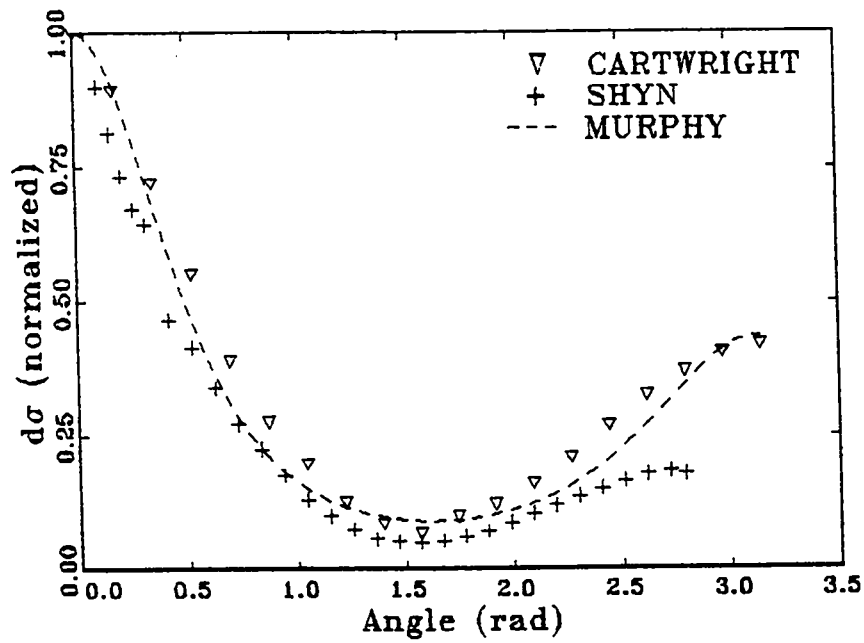

Figure 24: Elastic differential cross section at 15 eV.

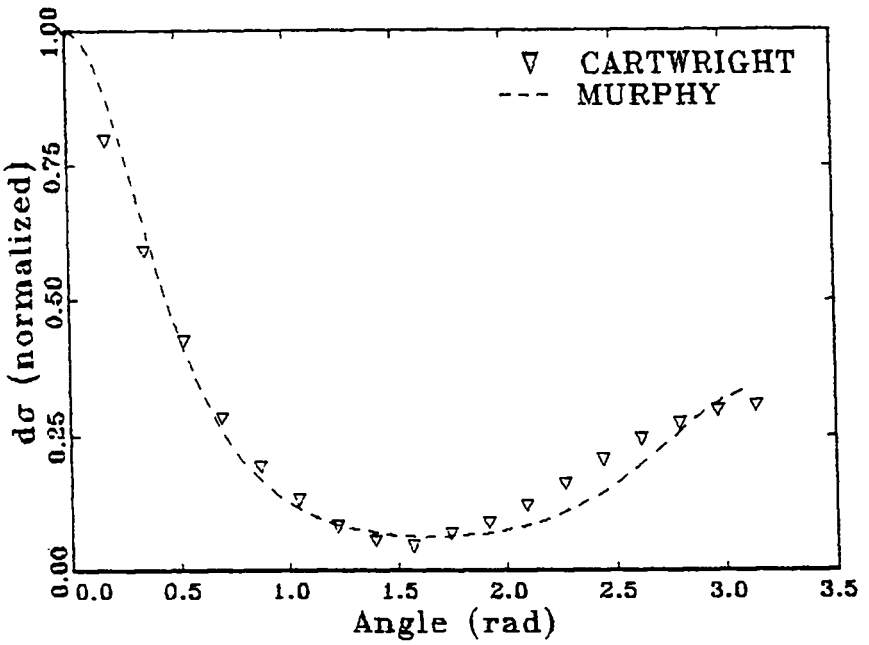

Figure 25: Elastic differential cross section at 17 eV.

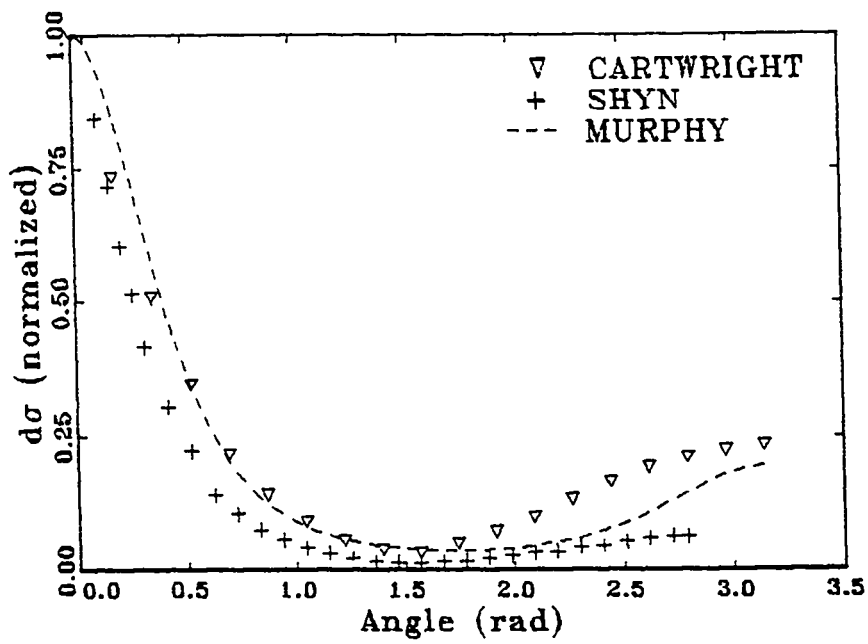

Figure 26: Elastic differential cross section at 20 eV.

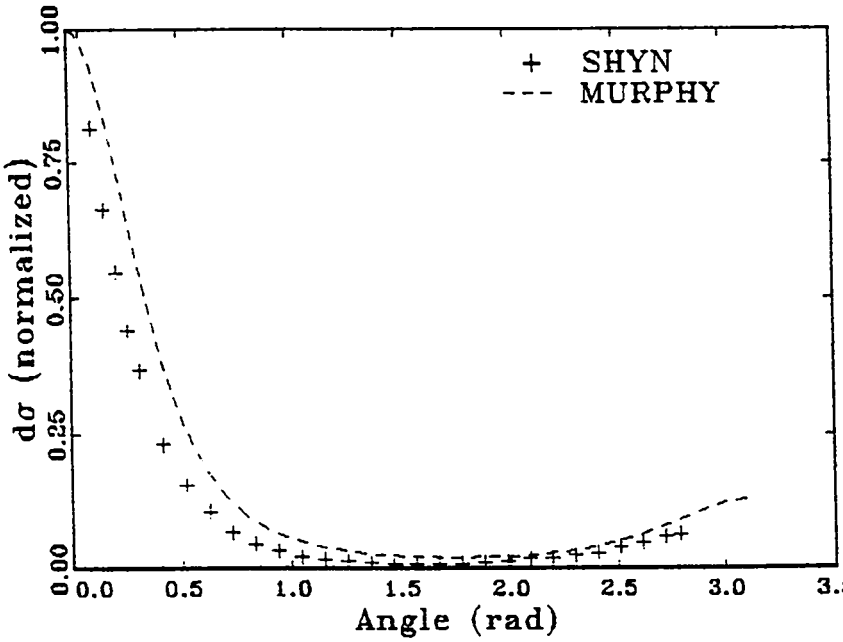

Figure 27: Elastic differential cross section at 25 eV.

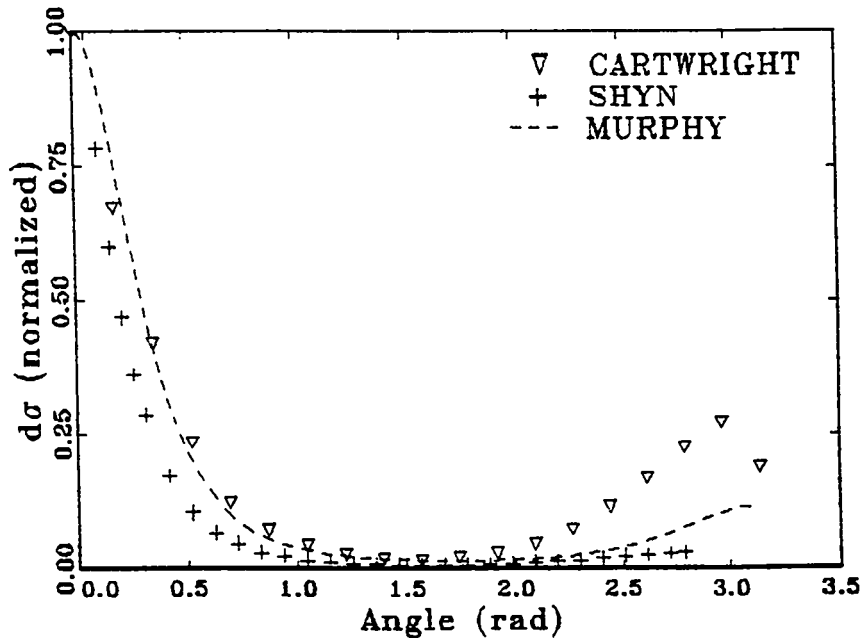

Figure 28: Elastic differential cross section at 30 eV.

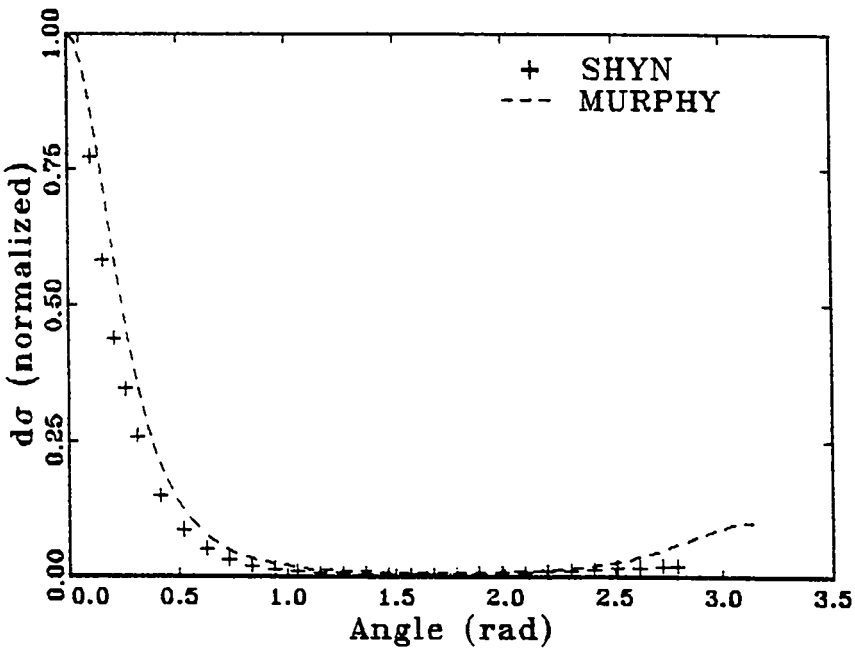

Figure 29: Elastic differential cross section at 40 eV.

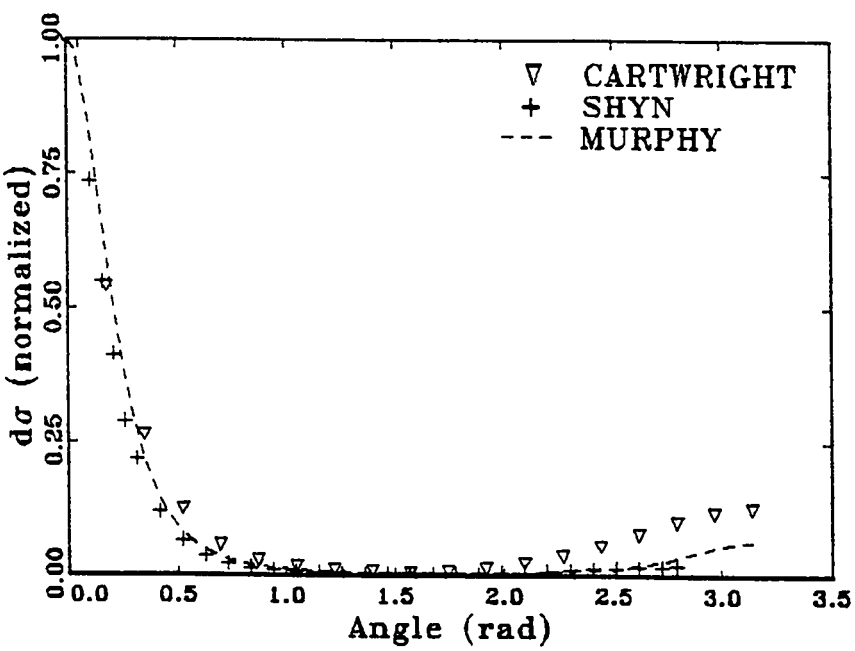

Figure 30: Elastic differential cross section at 50 eV.

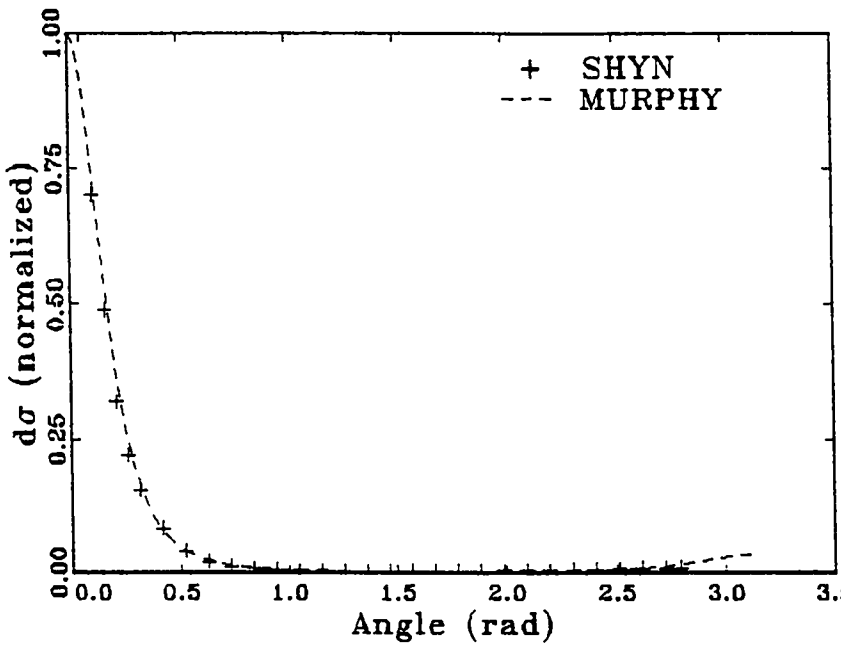

Figure 31: Elastic differential cross section at 70 eV.

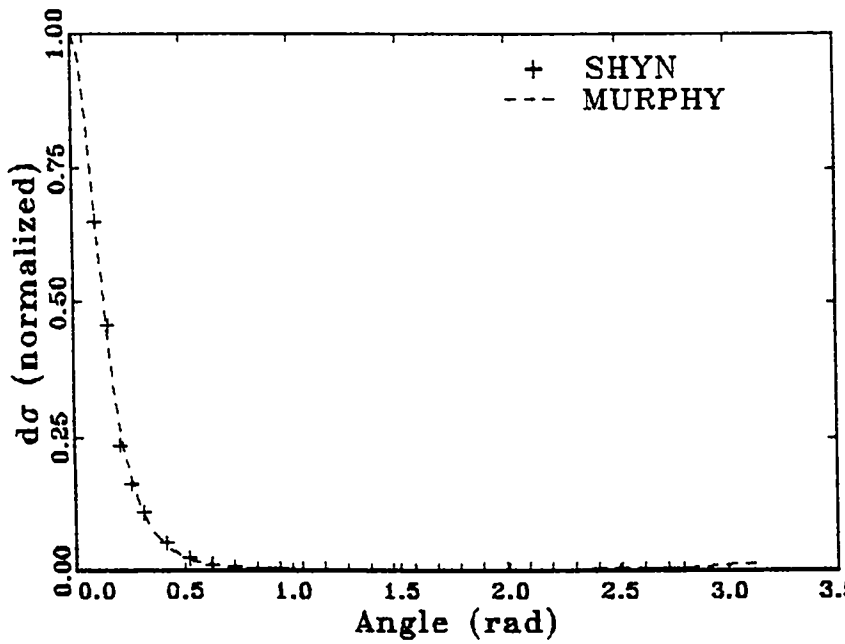

Figure 32: Elastic differential cross section at 90 eV.

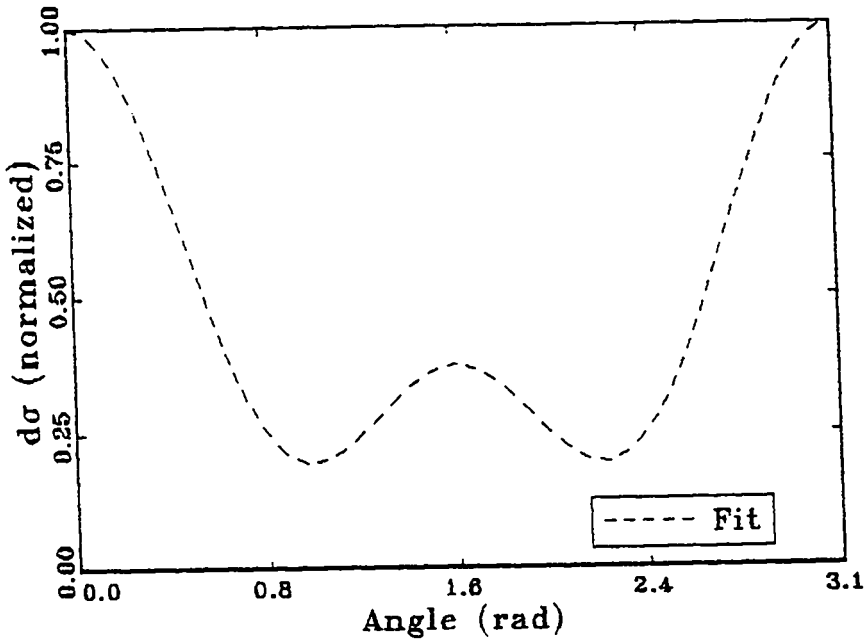

Figure 33: Vibrational and rotational differential cross section at 2 eV.

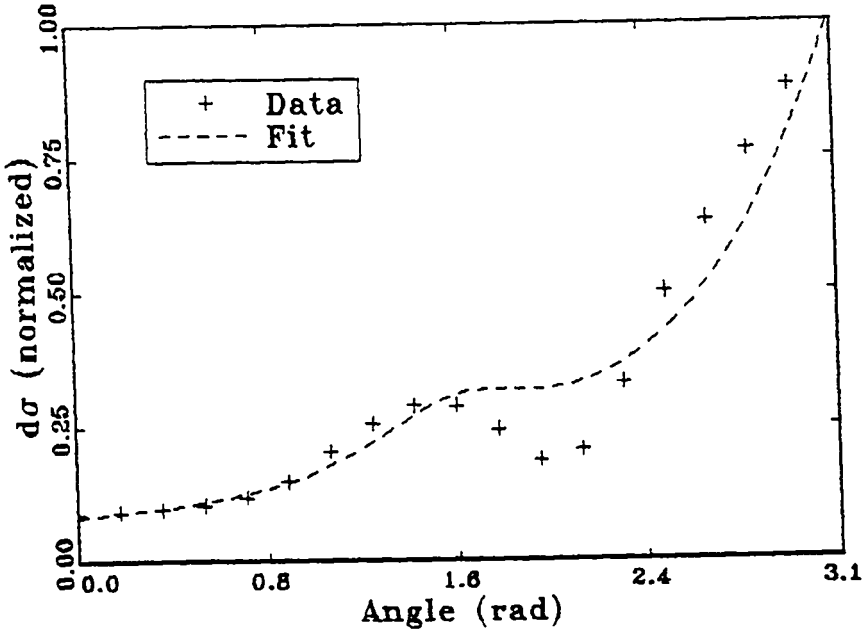

Figure 34: Electronic $A^3\Sigma_u^+$ differential cross section at 17 eV.

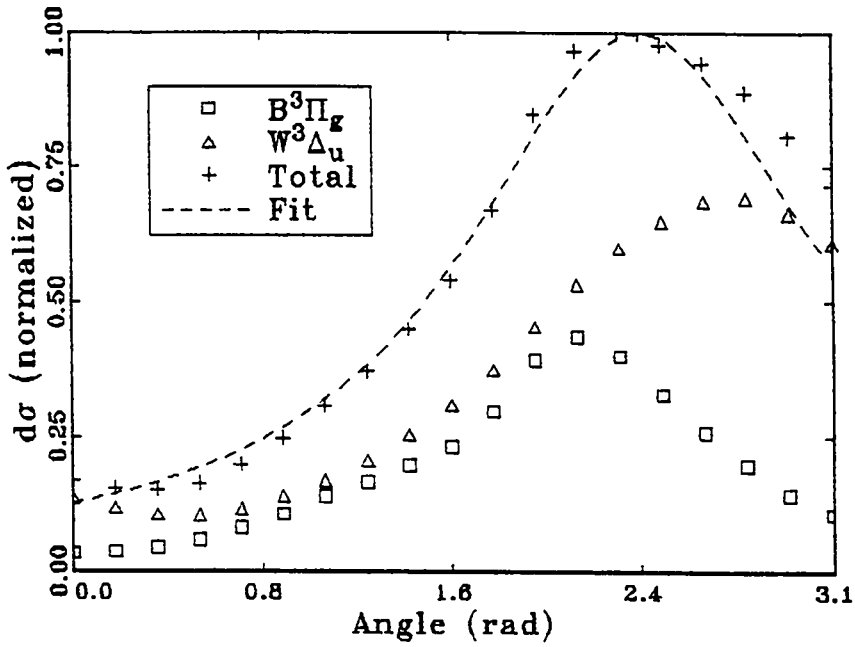

Figure 35: Electronic $B^3\Pi_g + W^3\Delta_u$ differential cross section at 15 eV.

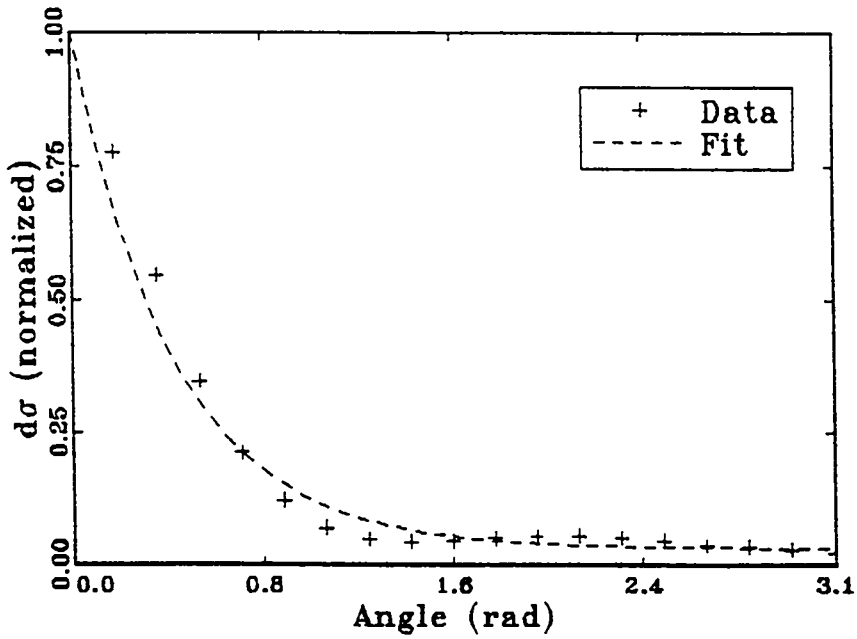

Figure 36: Electronic $a^1\Pi_g$ differential cross section at 17 eV.

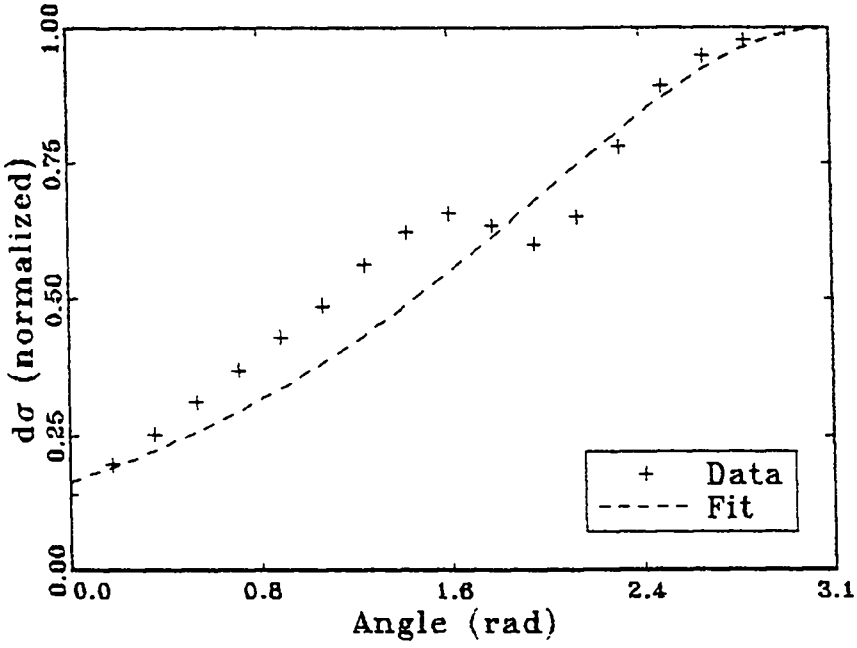

Figure 37: Electronic $C^3\Pi_u$ differential cross section at 15 eV.

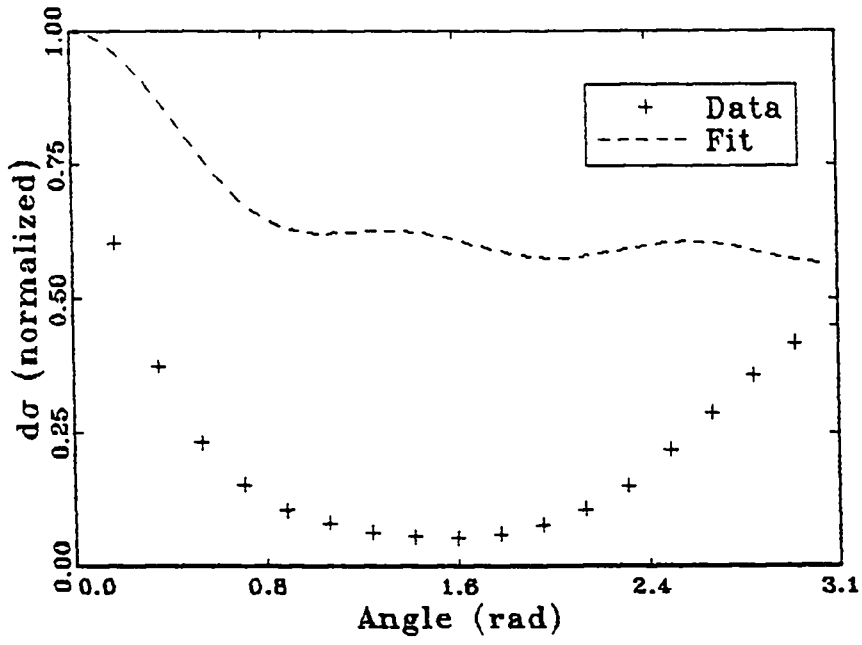

Figure 38: Rydberg differential cross section at 20 eV.

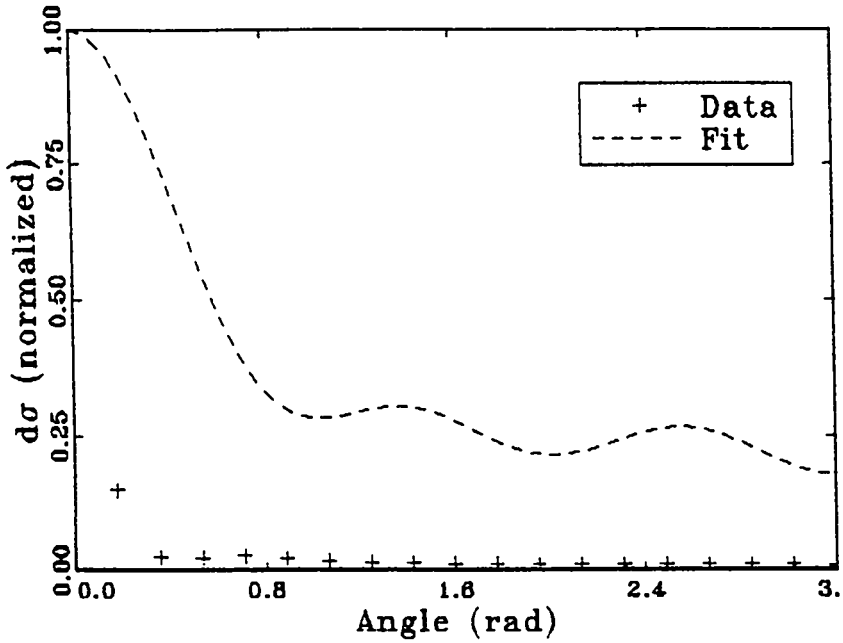

Figure 39: Rydberg differential cross section at 50 eV.

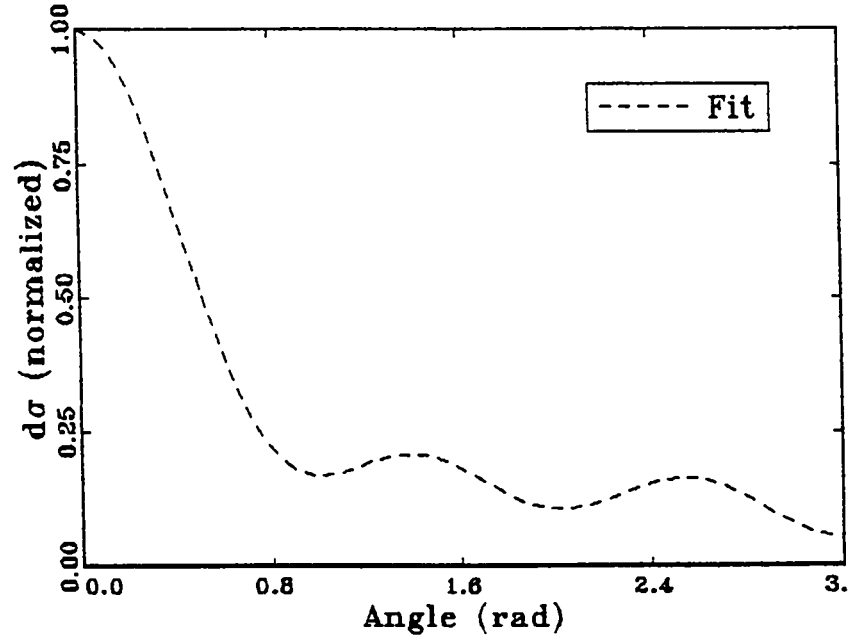

Figure 40: Rydberg differential cross section at 100 eV.

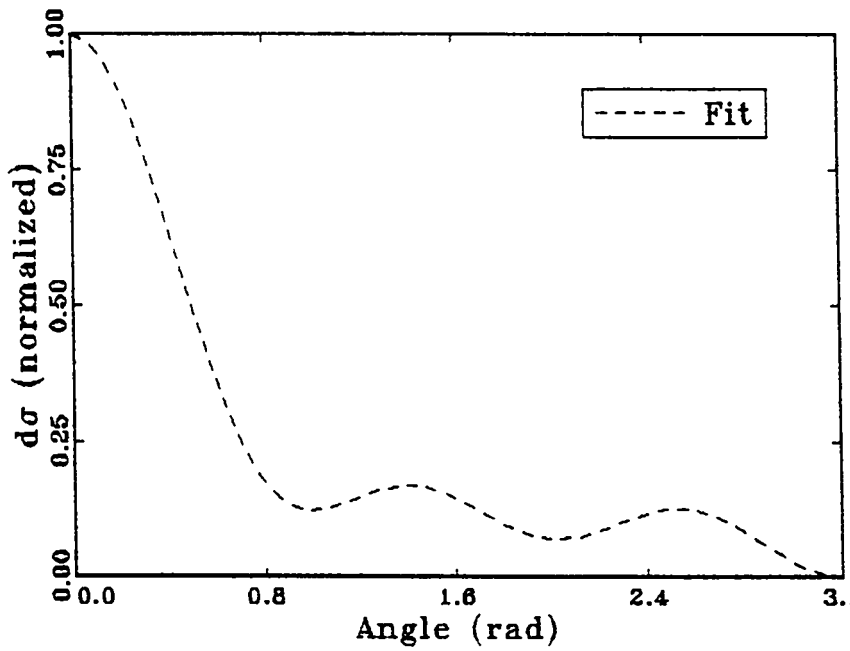

Figure 41: Rydberg differential cross section at 1000 eV.

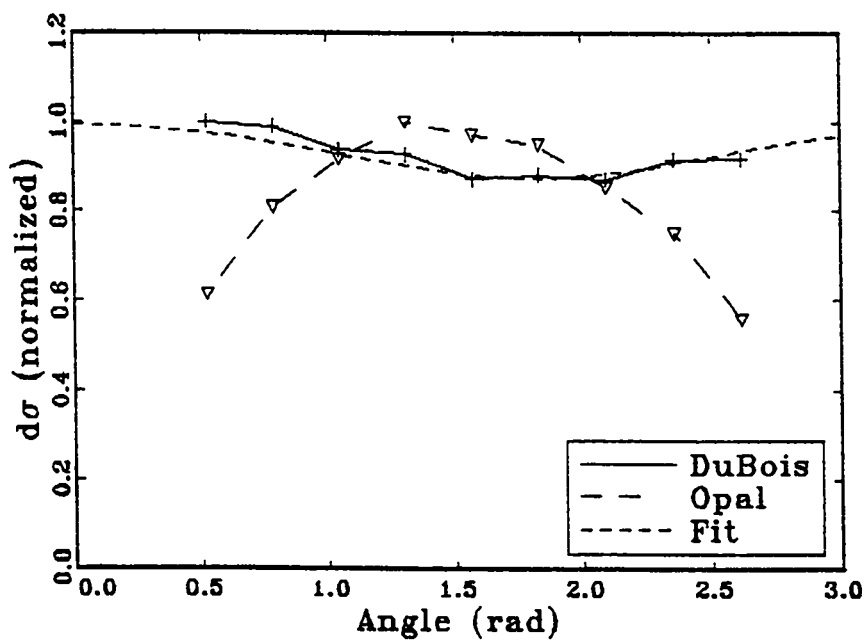

Figure 42: Ionization differential cross section at 4.13 eV.

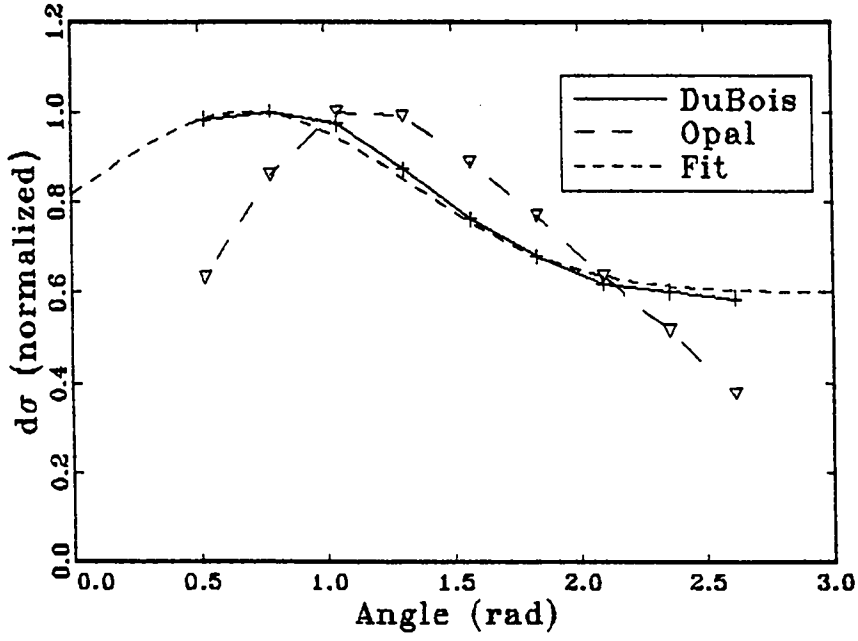

Figure 43: Ionization differential cross section at 20.1 eV.

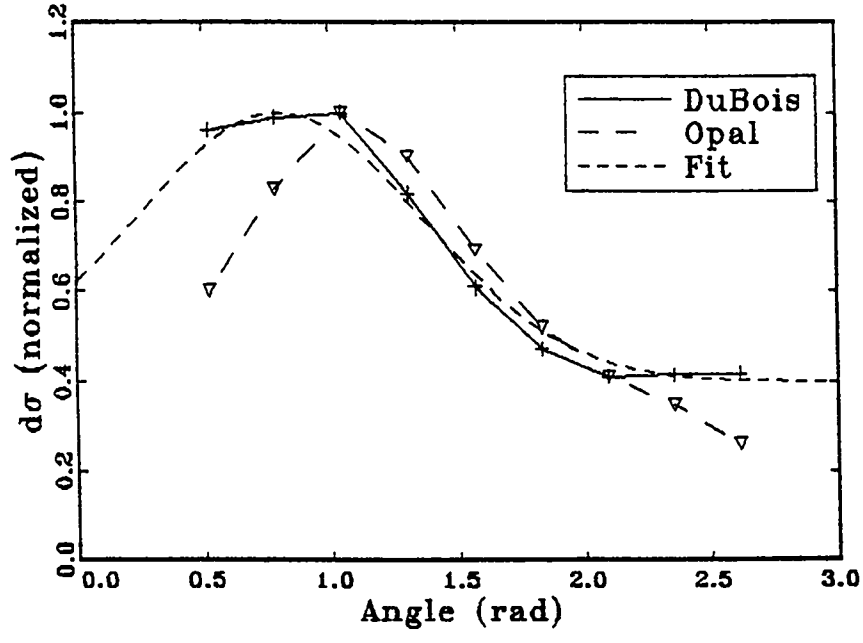

Figure 44: Ionization differential cross section at 48.5 eV.

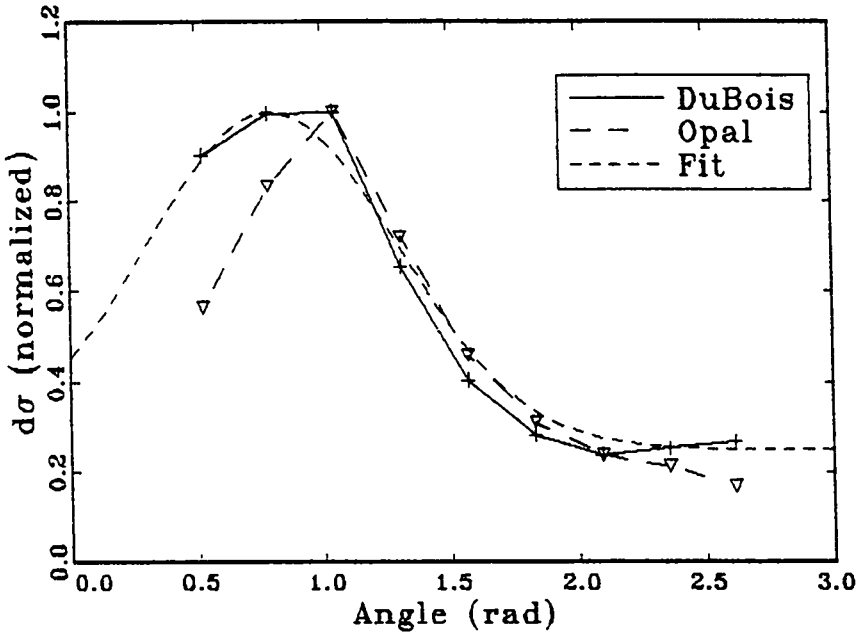

Figure 45: Ionization differential cross section at 98.0 eV.

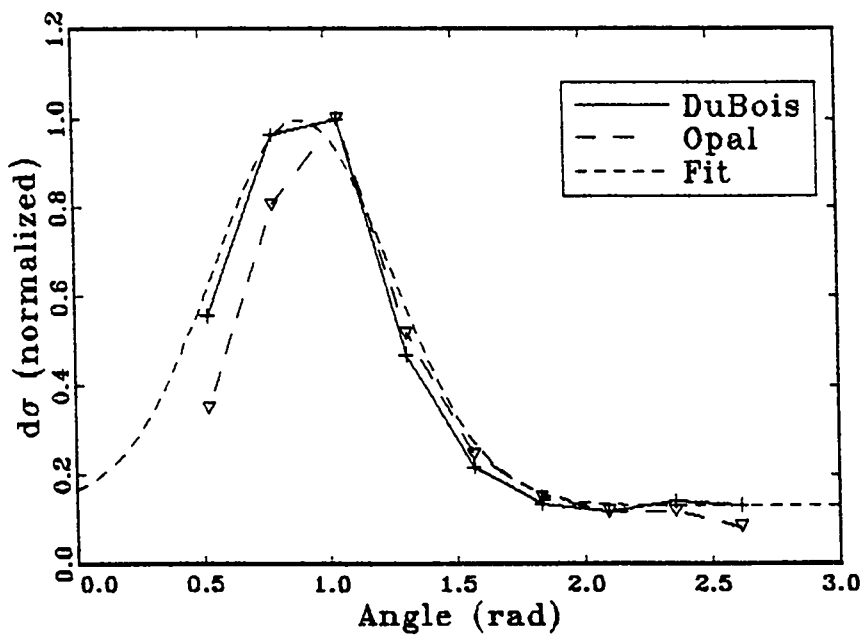

Figure 46: Ionization differential cross section at 196 eV.

References

[1] A.V. Phelps, JILA Rep. 28 (1985).

[2] A.V. Phelps and L.C. Pitchford, JILA Rep. 26 (1985).

[3] J.H. Jacob, Phys. Rev. A 8, 226 (1973).

[4] P.M. Banks and G. Kockarts, *Aeronomy*, Academic Press, New York, 1973, p. 201.

[5] D.C. Cartwright, A. Chutjian, S. Trajmar, and W. Williams, Phys. Rev. A 16, 1041 (1977).

[6] D. Rapp and P. Englander-Golden, J. Chem. Phys. 43, 1464 (1965).

[7] C.B. Opal, E.C. Beaty, and W.K. Peterson, J. Chem. Phys. 55, 4100 (1971).

[8] C.B. Opal, E.C. Beaty, and W.K. Peterson, At. Data 4, 210 (1972).

[9] C.L. Longmire and H.J. Longley, DNA 3192T (1973).

[10] H.A. Bethe, Ann. Phys. 5, 325 (1930).

[11] T.W. Shyn, R.S. Stolarski, and G.R. Carignan, Phys. Rev. A 6, 1002 (1972).

[12] S.F. Wong and L. Dubé, Phys. Rev. A 17, 570 (1977).

[13] L.S. Polak and D.I. Slovetskii, Teplofiz. Vys. Temp. 10, 645 (1972).

[14] D.C. Cartwright, A. Chutjian, S. Trajmar, and W. Williams, Phys. Rev. A 16, 1013 (1977).

[15] A.V. Phelps and L.A. Pitchford, Phys. Rev. A 31, 2932 (1985).

[16] R.D. DuBois and M.E. Rudd, Phys. Rev. A 17, 843 (1978).

Printed in the United States of America
Available from
National Technical Information Service
US Department of Commerce
5285 Port Royal Road
Springfield, VA 22161

Microfiche (A01)

Page Range	NTIS Price Code	Page Range	NTIS Price Code	Page Range	NTIS Price Code	Page Range	NTIS Price Code
001-025	A02	151-175	A08	301-325	A14	451-475	A20
026-050	A03	176-200	A09	326-350	A15	476-500	A21
051-075	A04	201-225	A10	351-375	A16	501-525	A22
076-100	A05	226-250	A11	376-400	A17	526-550	A23
101-125	A06	251-275	A12	401-425	A18	551-575	A24
126-150	A07	276-300	A13	426-450	A19	576-600	A25
						601-up*	A99

*Contact NTIS for a price quote.

Los Alamos National Laboratory
Los Alamos,New Mexico 87545